European Journal of Medicinal Chemistry 170 (2019) 126–140

Contents lists available at ScienceDirect

European Journal of Medicinal Chemistry

journal homepage: http://www.elsevier.com/locate/ejmech

Research paper

Evaluation of synthetic substituted 1,2-dioxanes as novel agents against human leishmaniasis

M. Ortalli [a, 1], S. Varani [a, b, 1], C. Rosso [c], A. Quintavalla [c, *], M. Lombardo [c], C. Trombini [c, **]

[a] Alma Mater Studiorum - University of Bologna, Department of Experimental, Diagnostic and Specialty Medicine, Via Massarenti 9, 40138, Bologna, Italy
[b] Unit of Clinical Microbiology, Regional Reference Centre for Microbiological Emergencies (CRREM), St. Orsola-Malpighi University Hospital, Via Massarenti 9, 40138, Bologna, Italy
[c] Alma Mater Studiorum - University of Bologna, Department of Chemistry "G. Ciamician", Via Selmi 2, 40126, Bologna, Italy

ARTICLE INFO

Article history:
Received 22 November 2018
Received in revised form
29 January 2019
Accepted 25 February 2019
Available online 3 March 2019

Keywords:
Synthetic endoperoxides
Drug design
Leishmaniasis
Neglected tropical disease

ABSTRACT

The treatment of human leishmaniasis is currently based on few compounds that are highly toxic, expensive and have a high rate of treatment failure. A number of recent studies on new drugs focuses on natural or semi-synthetic compounds. Among them, the endoperoxide artemisinin, extracted from *Artemisia annua*, and some of its derivatives have shown leishmanicidal activity. In the present work, a series of structurally simple, fully synthetic 1,2-dioxanes were evaluated for *in vitro* antileishmanial activity against promastigotes of *Leishmania donovani;* the cytotoxicity for mammalian cells was also assessed. The six most promising compounds in terms of activity and selectivity were further investigated for their antileishmanial activity on the promastigote forms of *L. tropica, L. major* and *L. infantum* and against *L. donovani* amastigotes. The good performance in terms of potency and selectivity makes these six hits promising candidates for a preliminary lead optimization as antileishmanial agents.

1. Introduction

Human leishmaniasis is one of the most burdensome neglected tropical diseases, which is endemic in around 100 countries including Southern Europe, Asia, Africa, and Latin America, with more than 350 million people living at risk of developing one of the many forms of the disease [1]. *Leishmania* parasites are transmitted into mammalian host by the bite of phlebotomine sand flies (genus *Phlebotomus* in the Old World and *Lutzomyia* in the New World) as promastigotes (flagellates), that transform into aflagellated amastigotes in host macrophages [2]. Leishmaniasis is considered a neglected tropical disease and it is linked to poverty, but environmental and climate-related factors also influence the disease's epidemiology. In the last decades, probably due to global warming, long-distance tourism and trade, leishmaniasis has spread to countries, including industrialized countries, previously considered unsuitable for the proliferation of the vector and/or the parasite [3,4]. The clinical spectrum of human infection ranges from the life-threatening visceral disease (VL) characterized by fever, splenomegaly, pancytopenia and weight loss, to disfiguring mucosal (ML) and cutaneous (CL) forms, to asymptomatic infection [5].

The currently employed pharmacological approach to treat leishmaniases is based on few drugs including pentavalent antimonials (meglumine antimoniate and sodium stibogluconate), liposomial amphotericin B, paromomycin, miltefosine, pentamidine and sitamaquine (Fig. 1) [6]. Treatments are unsatisfactory in terms of safety and efficacy, which sharply contrasts with the therapeutic need in terms of people at risk, number of affected patients and associated fatalities. Indeed, many different toxic effects and adverse reactions are associated with the use of the currently employed drugs [6,7] and drug resistance is nowadays a serious problem in some endemic areas [8]. The recently introduced compounds and formulations display good efficacy, but the high costs and/or the low bioavailability limit in some cases their application [9].

Nowadays, leishmaniasis is still lacking an effective, safe, and affordable chemotherapy.

The several drawbacks shown by antileishmanial drugs, together with the worldwide high impact of leishmaniasis on the public health, prompt the scientific community to urgently identify new chemical entities able to act as effective, safe and cheap antileishmanial drugs [10,11].

* Corresponding author.
** Corresponding author.
E-mail address: arianna.quintavalla@unibo.it (A. Quintavalla).
[1] These authors equally contributed to this work.

https://doi.org/10.1016/j.ejmech.2019.02.070

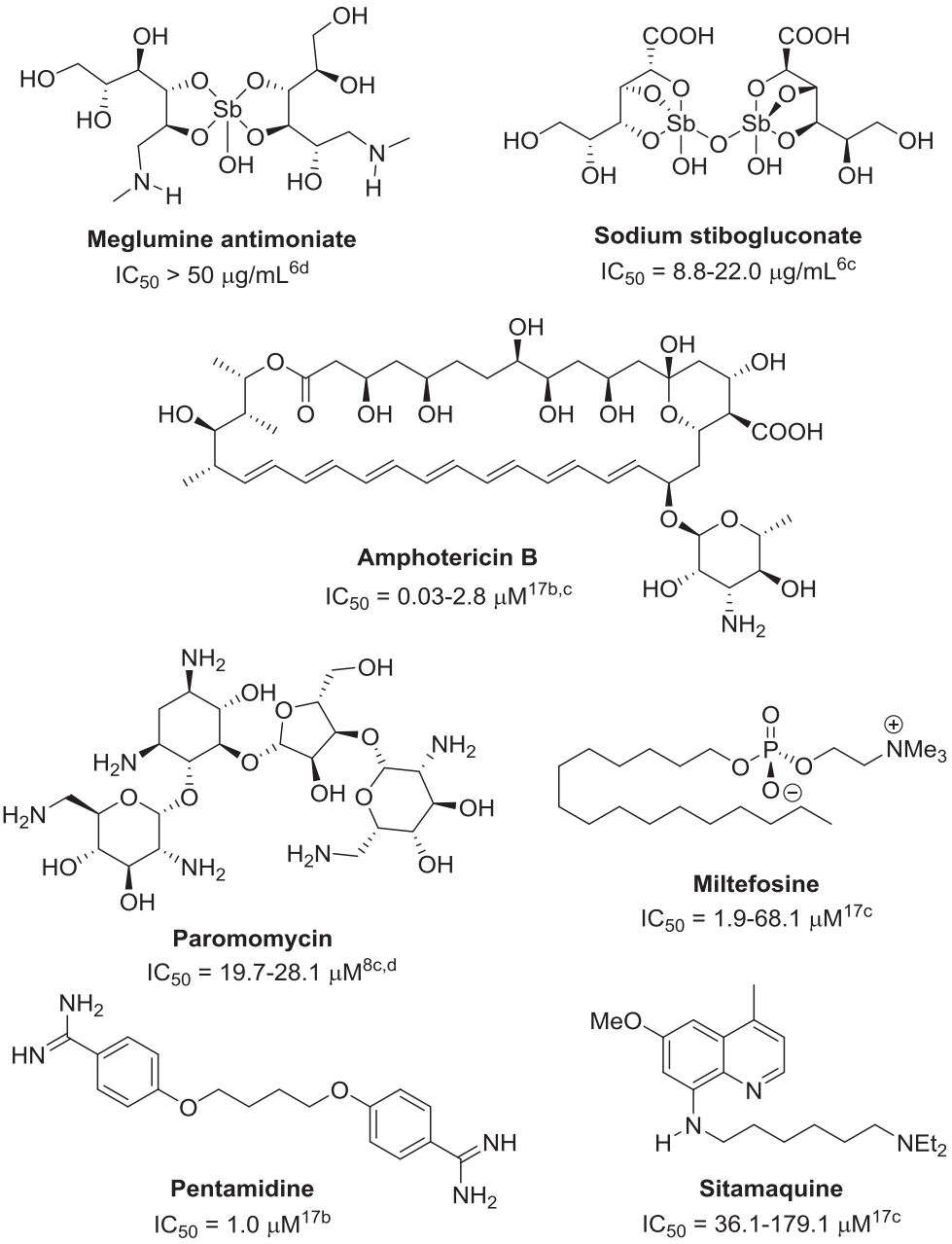

Fig. 1. Drugs currently employed for the treatment of leishmaniases (the reported IC_{50} values concern bioassays on promastigotes of *Leishmania donovani* strains).

In the broad field of antiparasitic compounds, promising activities are exhibited by plant-derived substances. In this context, the endoperoxide artemisinin and its derivatives (Fig. 2) play a crucial role, owning to a wide range of biological activities [12]. Artemisinin and some semi-synthetic derivatives, such as dihydroartemisinin or artesunate (Fig. 2), are the main components of artemisinin-based combination therapies (ACTs), recommended by the World Health Organization (WHO) as first-line treatment for *Plasmodium falciparum* malaria in disease-endemic countries [13]. In addition, artemisinin-based compounds revealed to be active as antimicrobial [14] and antiviral agents [15]. Furthermore, artemisinin derivatives display bioactivity also against non-malarial protozoa that infect humans, such as *Leishmania* spp. and *Trypanosoma* spp [12].

Concerning the *Leishmania* treatment, one of the most relevant features of the artemisinin-derived endoperoxides is the ability to inhibit the parasite metabolism with limited adverse effects on the host cells [16]. Studies were carried out on the activity of artemisinin derivatives on *Leishmania* (Fig. 2), with varying IC_{50} values depending on the compound structure, the tested parasite species and the selected parasite form (promastigote or amastigote) (Fig. 2) [12,17].

It is noteworthy that the *in vitro* efficacy of some of these semi-synthetic cyclic peroxides is comparable to or, in some cases, higher than those of amphotericin B, miltefosine, and sitamaquine [12].

Among the endoperoxide-based scaffolds tested against *Leishmania* spp., the fully synthetic and structurally simple trioxolanes **LC50** and **LC95** (Fig. 2) display good bioactivity profiles when tested *in vitro* against promastigotes (IC_{50} range 3.51 μM–9.35 μM) and a modest activity against intracellular amastigotes (IC_{50} range

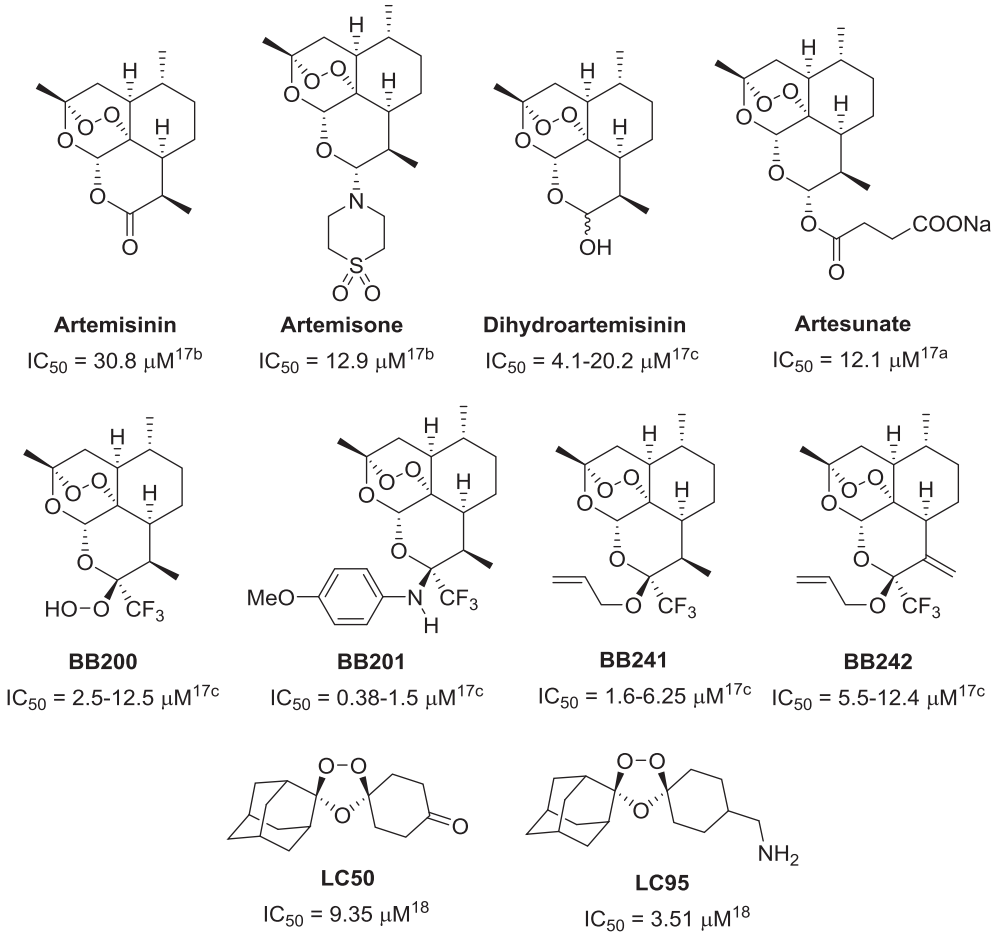

Fig. 2. Antileishmanial activity of some artemisinin derivatives and synthetic trioxolanes (the reported IC_{50} values concern bioassays on promastigotes of *L. donovani* for artemisinin derivatives and of *L. infantum* for trioxolanes).

79.76 μM–107.87 μM) of *L. infantum* [18]. Interestingly, some synthetic trioxolanes are more effective than dihydroartemisinin and artesunate, and show higher selectivity index (SI) values than those of commercially available antileishmanial drugs.

In the last years, part of our ongoing research work was focused on the design and synthesis of new antimalarial agents [19]. In details, we proposed an efficient and cheap synthetic strategy to assemble simple 3-methoxy-1,2-dioxanes 8 suitably decorated in position 4 and 6 (Scheme 1). Inspired by the good antileishmanial properties shown by some endoperoxide-containing scaffolds, such as artemisinin derivatives and trioxolanes (Fig. 2), we decided to test our 1,2-dioxanes library for antileishmanial activity and to design new and specifically substituted endoperoxides that could be able to act as antileishmanial compounds.

The objectives of the present study are: *i)* the development of an efficient protocol to synthesize new antileishmanial 1,2-dioxanes; *ii)* a preliminary investigation of the structure-activity relationships (SARs), *iii)* the identification of a possible pharmacophore model. The structural simplicity of the proposed 1,2-dioxanes and the ease of synthesis at low cost represent a major advantage over natural compounds, which are characterized by complex structures that are only marginally modifiable. Indeed, we are able to obtain a family of variously substituted compounds, which allows us to identify the crucial pharmacophore molecular portions. In the long run we will focus our efforts to unravel the mechanism of action and the biological target of this family of anti-parasitic compounds.

2. Results and discussion

2.1. Synthesis of the first series of endoperoxides and in vitro inhibition of L. donovani promastigotes growth

A small library of 3-methoxy-1,2-dioxanes has been prepared through an efficient (up to 59% overall yield) and low cost synthetic approach developed in our lab [19]. The optimized protocol consists of five steps based on a key formal [2+2+2] free radical cycloaddition of a β-ketoester (**1**), a *gem*-disubstituted alkene (**2**) and molecular oxygen, promoted by catalytic amounts of manganese salts (Scheme 1). The obtained hemiketal (**3**) was first converted into the methylketal (**4**) and then reduced to the corresponding alcohol (**5**). Finally, an oxidation to aldehyde (**6**) followed by a reductive amination led to the desired substituted endoperoxide (**8**). The flexibility of the synthetic strategy enables the construction of several endoperoxides variously functionalized on the 3, 4 and 6 positions by simply varying the nature of the β-ketoester (**1**), the alkene (**2**) and the amine (**7**).

With this library of synthetic endoperoxides in hands, we evaluated the antileishmanial properties of 3-methoxy-1,2-dioxanes that previously showed the highest bioactivity as antimalarials, structurally characterized by the presence of an aminopropyl side-chain at 4-position and by a 3,4-*cis* stereochemistry. We started our investigation selecting *Leishmania donovani* as reference strain indicative of the leishmaniasis in the Old World. The bioactivity against the extracellular promastigote forms of *L. donovani*

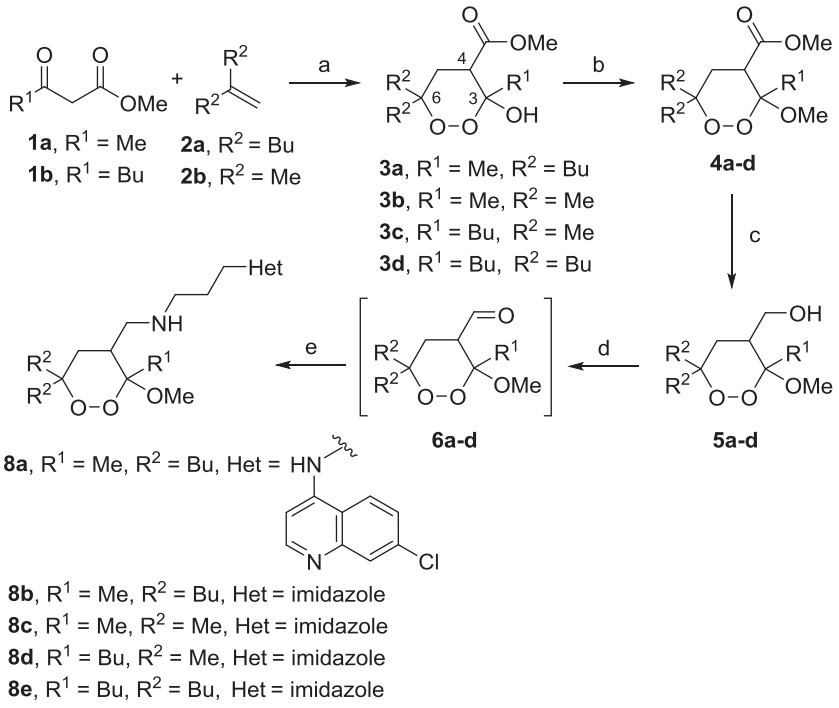

Scheme 1. Reagents and conditions: a) **1** (2 equiv.), $Mn(OAc)_3$ (5 mol%), $Mn(OAc)_2$ (5 mol%), O_2 (filled balloon), AcOH (3 mL/mmol), rt, 4–12 h (70–90%); b) CSA (15 mol%), MeOH (2 mL/mmol), reflux, 12–24 h (75–85%); c) DIBAL (2 equiv.), DCM (4 mL/mmol), −20 °C, 1 h (80–95%); d) Dess–Martin periodinane (1.3 equiv.), DCM (5 mL/mmol), rt, 1 h (80–90%); e) *i.* $Ar(CH_2)_3NH_2$ (**7**, 1 equiv.), MeOH (6 mL/mmol), rt, 5–7 h; *ii.* $NaBH_4$ (1.5 equiv.), 0 °C to rt, 1.5 h (80–90%, 2 steps). For more details on the synthesis see Ref. [19].

(MHOM/NP/02/BPK282/0cl4) was expressed as IC_{50}, *i.e.* the concentration of compound required to inhibit the parasite growth by 50% (Table 1). When an interesting bioactivity was observed, the corresponding cytotoxicity on Vero cells was also evaluated (Table 1). The collected data proved to be very interesting. The two different heteroaromatic systems (7-chloroquinolin-4-amine for **8a** and imidazole for **8b**) on the C4-side chain confer the corresponding endoperoxides a potent antileishmanial activity (IC_{50} range 1.6 μM–5.5 μM). In particular, the imidazole derivative **8b** displays a slightly lower potency, but also a significantly reduced cytotoxicity leading to a good selectivity index (SI = 13.5). Preserving the imidazole as the best substituent on C4, the nature of the alkyl groups at C3 and C6 was investigated, going from methyl to butyl. Compounds **8c** and **8d** with two methyl groups at C6 are inactive, suggesting that longer and more lipophilic substituents are needed in this position, regardless of the chain present at C3. Indeed, the tributyl derivative **8e** holds an IC_{50} value of 6.2 μM, comparable to that of the dibutyl derivative **8b**. However, the presence of a butyl at C3, instead of a methyl, seems to significantly increase the cytotoxicity (CC_{50} = 32.5 μM).

The antileishmanial activity on *L. donovani* promastigotes was also studied for the intermediates **3a**, **4a** and **5a**, obtained in the synthesis of the aminopropyl imidazole derivative **8b**, which showed the most promising bioactivity. The hemiketal **3a**, the ketal **4a** (both the isomers 3,4-*cis* and 3,4-*trans*), and the alcohol **5a** (both the isomers 3,4-*cis* and 3,4-*trans*) revealed to be all inactive at the tested concentration (Table 1). These findings demonstrate the crucial role played by the nature of the C4-side chain in determining the antileishmanial activity.

Finally, we tested the natural endoperoxide artemisinin and its semi-synthetic derivative artesunate on *L. donovani* promastigotes (Table 1). They displayed no antileishmanial activity under our bioassay conditions (40 μM of peroxide, promastigote forms of *L. donovani* MHOM/NP/02/BPK282/0cl4). These results are in agreement with some data reported in the literature for these compounds (artemisinin: IC_{50} = 100–160 μM [16a, 20]; artesunate: no cell death at 100 μg/mL [21]). These data allow us to infer that our synthetic, structurally simple compounds, *i.e.* 3-methoxy-1,2-dioxanes, display an excellent antileishmanial potency on *L. donovani*, compared to natural artemisinin and its semi-synthetic derivative artesunate. Indeed, the IC_{50} values on *L. donovani* promastigotes recorded for our endoperoxides are comparable to those of the most active antileishmanial artemisinin derivatives **BB200**–**201** and **BB241**–**242** (Fig. 2). Moreover, to the best of our knowledge, we present here the first study on the antileishmanial activity of fully synthetic endoperoxides on *L. donovani*, whereas the trioxolanes reported in Fig. 2 have been tested only on *L. infantum* [18].

2.2. Synthesis of the second series of endoperoxides and in vitro susceptibility tests against L. donovani promastigotes

Prompted by the first good bioactivity results obtained for 4-aminopropyl-substituted 3-methoxy-1,2-dioxanes (**8a**, **8b**, and **8e**; Table 1) and on the basis of the preliminary structure-activity relationships (SARs) emerged, we designed some new endoperoxides to be tested against *L. donovani* promastigotes. In particular, we planned the following structural modifications: i) replacement of the imidazole with a triazole (**8f**, Scheme 2), to investigate the impact of the heteroaromatic system; ii) replacement of the butyl chains on C6 with phenyl groups (**8g-i**, Scheme 2) or a group derived from β-pinene (**8j-k**, Scheme 2), to vary the lipophilic properties of the endoperoxides; iii) insertion of a fluconazole-type moiety on C4-side chain (**8m**, Scheme 2), being fluconazole an antifungal drug also active against some *Leishmania* spp. [22]; iv) introduction of a phosphonium salt on the C4-side chain (**8n-q**, Scheme 2), a group that is known to direct bioactive molecules to mitochondria [23]. Finally, we decided also to evaluate the effect of

Table 1
Inhibitory activity of the first series of endoperoxides against promastigotes of *L. donovani*, cytotoxicity in mammalian kidney epithelial cells (Vero) and selectivity indexes.

Compound[a]	*L. donovani* promastigotes IC_{50} (μM)[b]	Vero CC_{50} (μM)[c]	SI[d]
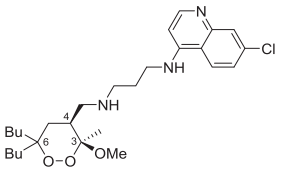 **8a**	1.6	4.0	2.5
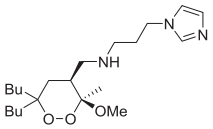 **8b**	5.5	74.5	13.5
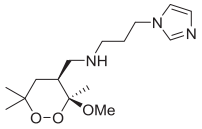 **8c**	> 40	nd	nd
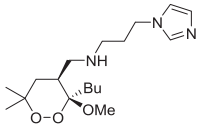 **8d**	> 40	nd	nd
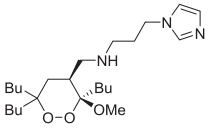 **8e**	6.2	32.5	5.2
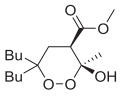 **3a**	> 40	nd	nd
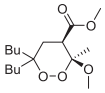 ***cis*-4a**	> 40	nd	nd
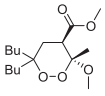 ***trans*-4a**	> 40	nd	nd
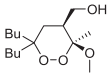 ***cis*-5a**	> 40	nd	nd
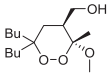 ***trans*-5a**	> 40	nd	nd
Artemisinin	> 40	nd	nd
Artesunate	> 40	nd	nd
Amphotericin B	0.3	200.0	666.7

[a] Compounds tested as racemates.
[b] IC_{50} represents the concentration of a compound that causes 50% growth inhibition. The experimental error was in the range 1–2.5 μM. See Supporting Information for details.
[c] CC_{50} represents 50% cytotoxic concentration on Vero cells.
[d] Selectivity index (SI) = CC_{50}/IC_{50}. nd = not determined due to the low antileishmanial potency.

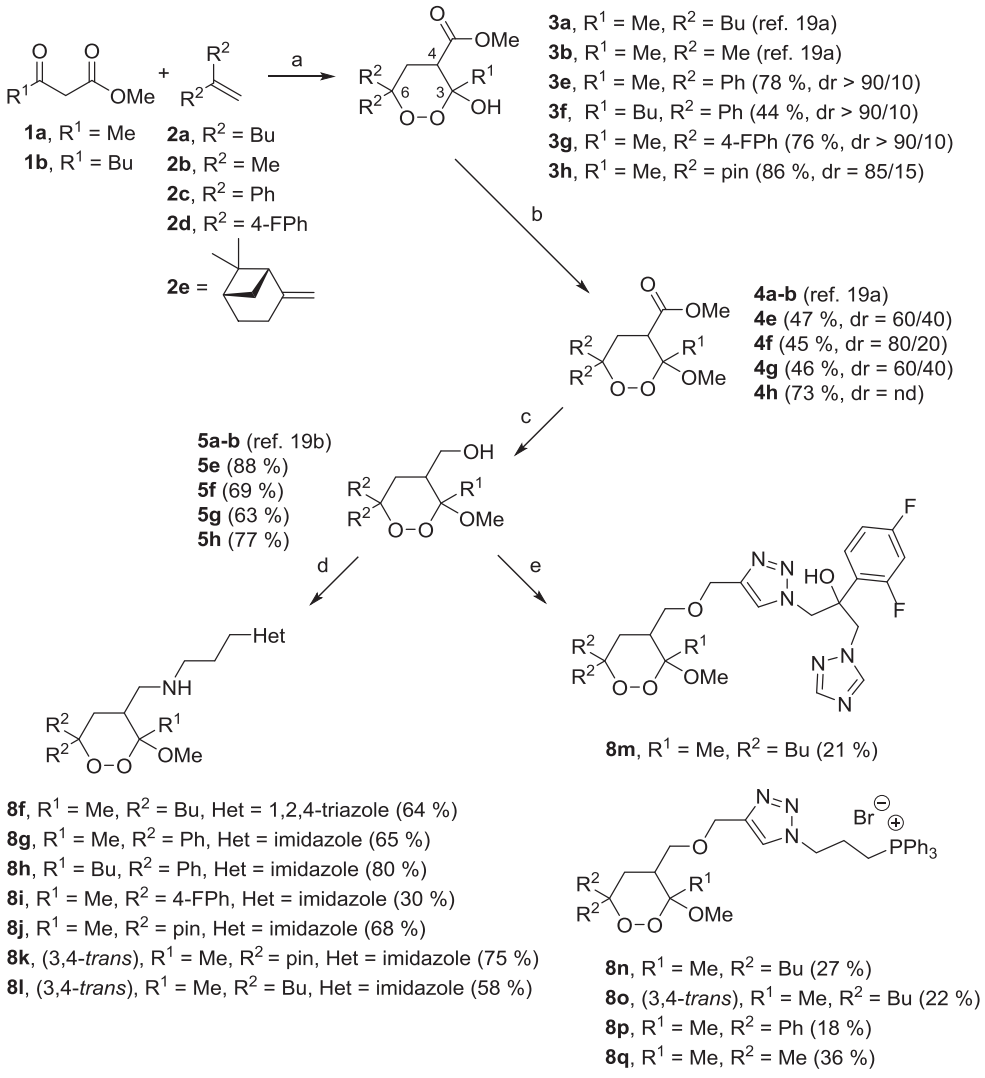

Scheme 2. Reagents and conditions: a) **1** (2 equiv.), $Mn(OAc)_3$ (5 mol%), $Mn(OAc)_2$ (5 mol%), O_2 (filled balloon), AcOH (3 mL/mmol), rt, 4 h; b) CSA (15 mol%), MeOH (2 mL/mmol), reflux, 24 h; c) $LiAlH_4$ (1 equiv.), THF (5 mL/mmol), 0 °C, 1 h; d) i. Dess–Martin periodinane (1.2 equiv.), DCM (5 mL/mmol), 0 °C to rt, 1 h; ii. amine (**7**, 1 equiv.), MeOH (6 mL/mmol), rt, overnight; iii. $NaBH_4$ (1.5 equiv.), 0 °C to rt, 1.5 h (overall yields reported); e) i. NaH (1.1 equiv.), propargyl bromide (1.2 equiv.), THF (5.5 mL/mmol), 0 °C to rt, overnight; ii. azide (**10**, 1 equiv.), $Cu(PPh_3)_3Br$ (10 mol%), DCM (16 mL/mmol), rt, overnight (overall yields reported). dr indicates 3,4-*cis*/3,4-*trans* ratio. pin = pinene-derived scaffold. nd = not determined due to the complexity of the reaction mixture. Unless noted otherwise, the final products **8** show 3,4-*cis* stereochemistry.

the endoperoxides relative stereochemistry on the activity, testing some 3,4-*trans* analogues (**8k**, **8l**, and **8o**, Scheme 2).

The new designed compounds were synthesized initially by exploiting the already optimized strategy leading to the alcohol **5** (Scheme 2). This product served as common intermediate to approach both new aminopropyl derivatives (**8f-l**, Scheme 2) through an oxidation/reductive amination sequence, and the new triazolyl ethers (**8m-q**, Scheme 2) through an alkylation/click cycloaddition sequence.

The Mn-promoted cycloaddition applied to the selected substrates **1** and **2** provided the desired new hemiketals **3e-h** with good yields (step a, Scheme 2), except for **3f** which displayed poor solubility and a difficult purification. The process showed in all the examples a marked diastereoselectivity in favor of the 3,4-*cis* isomers. The ketalization step generally proceeded with yields around 50% (step b, Scheme 2) and afforded two C3 epimers, also when using a pure *cis* hemiketal as the starting material. The key intermediate alcohols **5** were obtained in good yields through a chemoselective ester reduction (step c, Scheme 2) not affecting the endoperoxide O–O bond. Usually, the ketalization and the reduction steps were carried out on mixtures of 3,4-*cis*/3,4-*trans* endoperoxides, then the two C3-epimers of **5** were easily separated by flash chromatography. Starting from **5**, the two series of products **8** were synthesized. Exploiting the oxidation/reductive amination sequence (step d, Scheme 2), the aminopropyl derivatives (**8f-l**) were isolated in good to high overall yields. The second family of designed endoperoxides, characterized by an ether and a triazole as linker (**8m-q**, Scheme 2), was obtained through an alkylation reaction followed by a click cycloaddition (step e, Scheme 2), displaying both moderate yields. However, no further optimizations were carried out for these reactions, since the desired products were obtained pure in sufficient amounts to be assayed and fully characterized.

The new twelve endoperoxides (**8f-q**) were tested on promastigotes of *L. donovani* and the corresponding cytotoxicity on Vero cells was evaluated for compounds showing antileishmanial activity (Table 2).

The replacement of imidazole with 1,2,4-triazole in the C4-side

Table 2
Inhibitory activity of the second series of endoperoxides against promastigotes of *L. donovani*, cytotoxicity in mammalian kidney epithelial cells (Vero) and selectivity indexes.

Compound[a]	*L. donovani* promastigotes IC_{50} (μM)[b]	Vero CC_{50} (μM)[c]	SI[d]
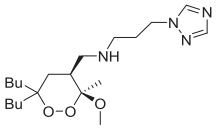 8**f**	> 40	nd	nd
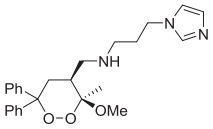 8g	7.5	50.0	6.7
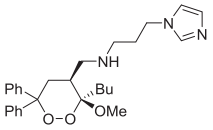 8h	4.2	9.5	2.3
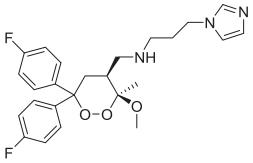 8i	12.0	93.6	7.8
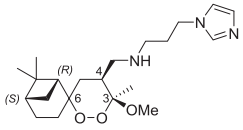 8j[e]	16.3	274.3	16.8
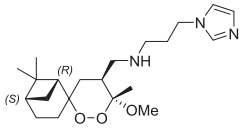 8k-A[f]	16.4	300.0	18.3
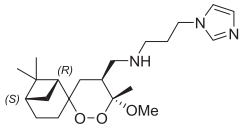 8k-B[f]	8.0	276.5	34.6
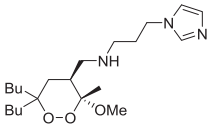 8l	4.0	140.0	35.0
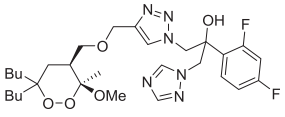 8m	16.0	195.0	12.2
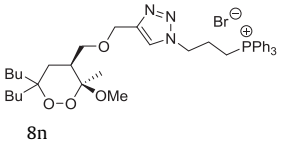 8n	15.5	102.0	6.6
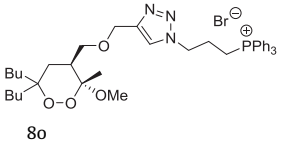 8o	40.0	200.0	5.0

Table 2 (*continued*)

Compound[a]	*L. donovani* promastigotes IC_{50} (μM)[b]	Vero CC_{50} (μM)[c]	SI[d]
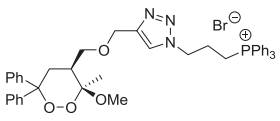 8p	11.5	280.0	24.3
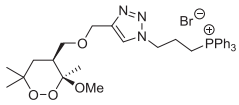 8q	> 40	nd	nd
Fluconazole	> 40	nd	nd

[a] Except for pinene-derivatives, the compounds were tested as racemates.
[b] IC_{50} represents the concentration of a compound that causes 50% growth inhibition. The experimental error was in the range 1–2.5 μM. See Supporting Information for details.
[c] CC_{50} represents 50% cytotoxic concentration.
[d] Selectivity index (SI) = CC_{50}/IC_{50}.
[e] Mixture of 3,4-*cis* diastereoisomers.
[f] Mixture of 3,4-*trans* diastereoisomers. nd = not determined due to the low antileishmanial potency.

chain causes a complete loss of the antileishmanial activity (**8b**, Table 1 vs. **8f**, Table 2) confirming the crucial pharmacophoric role played by an imidazole ring in this position. The presence of phenyl groups instead of butyl chains on C6 does not affect bioactivity [24] (**8b**, Table 1 vs. **8g**, Table 2) whereas the cytotoxicity resulted slightly increased (CC_{50} = 50 μM), with a halved selectivity index. As already noticed for C6-butyl derivatives (**8b** and **8e**, Table 1), also for C6-phenyl derivatives the introduction of a butyl at C3 significantly enhances the cytotoxicity (**8h** vs. **8g**, Table 2). Minor consequences on both activity and selectivity are observed by inserting a *para*-F substituent on C6-phenyl rings (**8i** vs. **8g**, Table 2). On the C6 position of the endoperoxide, we evaluated also the presence of the bicyclic system derived from beta-pinene ((1*S*,5*S*)-2(10)-pinene) (**8j-k**, Table 2). In this case, the synthetic strategy led to the formation of a further stereocenter at C6 and the products were obtained as complex mixtures of stereoisomers (eight diastereoisomers formed). We were able to separate the four 3,4-*cis* isomers (**8j**) from the four 3,4-*trans* ones (**8k**), but the products **8j** and **8k** were assayed as mixture of isomers. Moreover, we tested two fractions of the 3,4-*trans* derivative **8k** (**8k-A** and **8k-B**) characterized by a different isomers composition. The antileishmanial properties of all the pinene derivatives are good and their cytotoxicity is particularly low. The best result was recorded for 3,4-*trans* **8k-B** displaying IC_{50} value of 8 μM, CC_{50} value of 276.5 μM and SI of 34.6. The higher activity of **8k-B** compared to **8k-A** demonstrates that some 3,4-*trans* isomers are more potent than others. Therefore, further investigations are currently underway in our laboratory to separate the diastereomeric mixtures and to identify the most potent scaffolds.

Replacement of butyl chains at C6 with both phenyl groups (**8g-i**) or the pinene-derived scaffold (**8j-k**) provides endoperoxides with good antileishmanial performances and it confirms that this class of compounds requires significant lipophilic substituents in this position.

With the aim to better understand the impact of the 3,4-relative stereochemistry on the bioactivity, we tested **8l**, the 3,4-*trans* analogue of one of the most active products (**8b**). **8l** displays an activity (IC_{50} = 4 μM) similar to the 3,4-*cis* analogue **8b**, but with a significantly improved selectivity (SI = 35), enough to become one of the best antileishmanial hit of this family.

Another structural modification we examined was the introduction on C4-side chain of a portion of the antifungal fluconazole. This moiety was bound to the endoperoxide through an ether linkage and one of the two 1,2,4-triazoles of fluconazole was replaced by a 1,2,3-triazole (**8m**, Scheme 2 and Table 2). The antileishmanial properties of this sort of hybrid product **8m** are good, similar to those of the corresponding imidazole derivative **8b** (Table 1), one of the lead compounds of the series. For comparison, we assayed also fluconazole on *L. donovani* promastigotes (Table 2) and the antifungal drug itself revealed to be inactive at the highest tested concentration (40 μM). This result suggests that the antileishmanial activity of fluconazole-inspired compound **8m** is related to the presence of both the endoperoxide system and of a suitable heteroaromatic ring system on the C4 side-chain.

The last group of new molecules reported in this article is characterized by a phosphonium salt on the C4-side chain bound through an ether/triazole linker (**8n-q**, Scheme 2 and Table 2). The purpose of introducing this peculiar ionic pendant was to investigate the possibility to direct our bioactive molecules to mitochondria [23]. The lipophilic cation was inserted on the core peroxide scaffolds bearing the most promising substituents on C3 (methyl) and on C6 (butyl, **8n-o**, and phenyl, **8p**). The phosphonium/butyl derivative **8n** (Table 2) is slightly less active and selective then the corresponding imidazole derivative **8b** (Table 1), although owns good antileishmanial properties. The corresponding 3,4-*trans* analogue **8o** is less effective than 3,4-*cis* **8n** (Table 2), in contrast to what displayed by diasteroisomers of the imidazole/butyl compounds **8b** and **8l** (Tables 1 and 2, respectively). The best behavior of the phosphonium-series was obtained for the phosphonium/phenyl derivative **8p** (Table 2). With IC_{50} = 11.5 μM, CC_{50} = 280 μM, and SI = 24.3, it revealed to be one of the most promising products of the family. For comparison, we synthesized and tested also the C6-methyl substituted compound **8q** (Scheme 2, Table 2). As previously observed for the corresponding imidazole/methyl derivative **8c** (Table 1), also the phosphonium/methyl derivative **8q** is inactive (Table 2), further confirming that: *i)* the C4-side chain alone does not provide an antileishmanial activity and that a suitable decorated endoperoxide moiety is required; *ii)* a lipophilic group longer than methyl must be present at C6, regardless of the nature of the C4-side chain.

Since we found that the phosphonium-substituted endoperoxides display a good antileishmanial bioactivity, further investigations are currently underway in order to verify whether mitochondria might be a biological target of our compounds.

Table 3
Comparison of inhibitory activity of compounds **8b**, **8l**, **8j**, **8k-B**, **8m**, **8p** against promastigotes of *L. donovani, L. major, L. tropica, L. infantum*.

Compound[a]	*L. donovani* promastigotes IC_{50} (μM)[b]	*L. major* promastigotes IC_{50} (μM)[b]	*L. tropica* promastigotes IC_{50} (μM)[b]	*L. infantum* promastigotes IC_{50} (μM)[b]
3,4-*cis* **8b**	5.5	11.8	8.9	3.0
3,4-*trans* **8l**	4.0	3.2	3.0	2.5
3,4-*cis* **8j**	16.3	15.5	35.0	6.0
3,4-*trans* **8k-B**	8.0	25.0	24.0	5.0
3,4-*cis* **8m**	16.0	38.4	38.0	12.0
3,4-*cis* **8p**	11.5	2.6	6.0	10.0

[a] Except for pinene-derivatives, the compounds were tested as racemates.
[b] IC_{50} represents the concentration of a compound that causes 50% growth inhibition. The experimental error was in the range 1–2.5 μM. See Supporting Information for details.

2.3. Evaluation of in vitro activity against L. tropica, L. major and L. infantumpromastigotes

The six most promising compounds in terms of activity and selectivity were further investigated for their antileishmanial efficacy on the promastigote forms of three other parasitic species, *i.e. L. tropica, L. major* and *L. infantum* (Table 3). In particular, we selected the most active products of the C4-imidazolyl series (3,4-*cis* **8b** and 3,4-*trans* **8l** C6-butyl derivatives; 3,4-*cis* **8j** and 3,4-*trans* **8k-B** C6-pinene derivatives), of the C4-phosphonium series (3,4-*cis* C6-phenyl derivative **8p**) and the fluconazole-inspired compound **8m**.

The products revealed to be active against all tested strains and the IC_{50} values are particularly low for *L. infantum*, ranging from 2.5 to 12 μM. The antileishmanial activity of C6-phenyl C4-phosphonium product **8p** are noticeable against *L. major* (IC_{50} 2.6 μM) and *L. tropica* (IC_{50} 6 μM). However, the most interesting bioactivity profile is shown by 3,4-*trans* C6-butyl C4-imidazole endoperoxide **8l**, which exhibits excellent performances against all the studied *Leishmania* strains (IC_{50} range from 2.5 to 4 μM).

2.4. Evaluation of in vitro activity against L. donovani amastigotes

Considering the promising results obtained, the structural features of **8b, 8l, 8j, 8k-B, 8p, 8m** were identified as crucial for the antileishmanial activity. Therefore, these compounds were selected to be tested for their efficacy against the amastigote stage of *L. donovani* that has pharmacological relevance because this form is specifically found in human cells (Table 4). The amastigote assay was performed by using metacyclic promastigotes to infect differentiated THP-1 macrophagic cells; amastigotes transformed from metacyclic promastigotes proliferated inside host macrophages.

In general, all the tested compounds exhibited a slightly higher inhibitory effect on promastigotes than on amastigotes, but it is noteworthy that the endoperoxides activity observed on promastigotes was preserved on amastigotes (Table 4). In fact, the very promising antileishmanial artemisinin derivatives **BB200**–**201** and **BB241**–**242** (Fig. 2), despite the high *in vitro* activity against *L. donovani* promastigotes, revealed to be inactive on intra-macrophage amastigote stage [17c]. Thus, these findings confirm that our synthetic endoperoxides are promising compounds for a pharmaceutical development.

In details, the promastigotes/amastigotes results are particularly similar for pinene-, fluconazole-, and phosphonium-derivatives (**8j-k**, **8m** and **8p**, respectively), whereas for the two isomers of butyl/imidazole scaffold (**8b** and **8l**) we observed a halved activity on amastigotes. However, we noticed that the best anti-amastigotes properties are displayed by the two 3,4-*trans* compounds **8l** and **8k-B**.

3. Conclusions

In order to identify novel antileishmanial agents, a library of 22 new and variously functionalized endoperoxides was synthetized and their antileishmanial activity was evaluated. Six compounds proved to be significantly active in *in vitro* assays against *L. donovani, L. tropica*, *L. major* and *L. infantum* promastigotes and against *L. donovani* amastigotes, with low cytotoxic effects towards mammalian cells. These six hits show an excellent performance in terms of potency and selectivity. Our findings suggest that the selected compounds act on biological targets specific for *Leishmania*, or that their internalization process is more efficient for parasitic cells rather than mammalian cells. Further investigations are underway to identify the parasite target/s.

Concerning the mechanism of action of endoperoxides, even if the exact mechanisms remains controversial, it is nowadays accepted that the role of endoperoxides against the malaria parasites involves the cleavage of O–O bond by Fe(II), leading to the generation of cytotoxic oxygen-centered radicals [25]. Plasmodial and leishmanial parasites exhibit some common features, such as the strong dependence on iron/heme supply by the mammalian host cell [26]. Evidences indicate that endoperoxides react rapidly with iron (II) resulting in the formation of oxygen- and carbon-centered radicals and impairing mitochondrial functions in parasites of the *Leishmania* genus [27]. In view of these studies, we speculate that the interaction with iron, the oxidative stress and the interference with the cellular respiration could represent one mechanism by which our synthetic endoperoxides act on *Leishmania*. Studies are currently underway in our laboratories to investigate the mechanism of action of these structurally simple

Table 4
Comparison of inhibitory activity of compounds **8b**, **8l**, **8j**, **8k-B**, **8m**, **8p** against promastigotes and amastigotes of *L. donovani*.

Compound[a]	*L. donovani* promastigotes IC_{50} (μM)[b]	*L. donovani* amastigotes IC_{50} (μM)[b]
3,4-*cis* **8b**	5.5	12.0
3,4-*trans* **8l**	4.0	10.3
3,4-*cis* **8j**	16.3	23.5
3,4-*trans* **8k-B**	8.0	9.7
3,4-*cis* **8m**	16.0	13.0
3,4-*cis* **8p**	11.5	15.0

[a] Except for pinene-derivatives, the compounds were tested as racemates.
[b] IC_{50} represents the concentration of a compound that causes 50% growth inhibition. The experimental error was in the range 1–2.5 μM. See Supporting Information for details.

endoperoxides.

In summary, in the reported study we demonstrated: *i)* the crucial pharmacophoric role played by the nature of the side-chain in the C4-position, being the aminopropyl imidazole and the triazolyl propyl phosphonium salt the two best substituents; *ii)* the significant lipophilic requirements at C6-position, with *n*-butyl, aryl and pinene-derived scaffold as best performing groups; *iii)* the need of a short (methyl) chain at C3-position to minimize the cytotoxicity. Furthermore, the good antileishmanial properties shown by the fluconazole-endoperoxide hybrid **8m** suggest that the observed bioactivity is related to the concurrent presence of the endoperoxide-system, being the antifungal drug itself inactive in our system.

The obtained results demonstrate that our synthetic and structurally simple 3-methoxy-1,2-dioxanes own a remarkable antileishmanial potency that is far superior to those of artemisinin and artesunate and comparable to the most active antileishmanial artemisinin derivatives **BB200**–**201**, **BB241**–**242** (Fig. 2).

It is noteworthy that the endoperoxide activity observed on *L. donovani* promastigotes was preserved on amastigotes (Table 4), thus confirming that this family of compounds can be pharmaceutically promising.

In conclusion, the excellent selective activity and the simple synthesis of endoperoxides **8b, 8l, 8j, 8k-B, 8p, 8m** highlight their potential as hits for lead optimization as antileishmanial agents.

4. Experimental methods

4.1. Chemistry

4.1.1. General information

All of the commercial chemicals were purchased from Sigma Aldrich, VWR, Alfa Aesar or TCI Chemicals, and used without additional purifications. The ^{1}H and ^{13}C NMR spectra were recorded on a 400 NMR instrument with a 5 mm probe. All chemical shifts have been quoted relative to deuterated solvent signals; chemical shifts (δ) are reported in ppm and coupling constants (J) are reported in Hertz. HPLC-LRMS analyses were performed on an Agilent Technologies HP1100 instrument coupled with an Agilent Technologies MSD1100 single-quadrupole mass spectrometer. A Phenomenex Gemini C18 3 μm (100 × 3 mm) column was employed for the chromatographic separation and two different analytical methods were used: *method A*: mobile phase H_2O/CH_3CN, gradient from 30% to 80% of CH_3CN in 8 min, 80% of CH_3CN until 22 min, then up to 90% of CH_3CN in 2 min, stop time at 25 min; flow rate 0.4 mL min^{-1}; *method B*: gradient analogous to method A employing a mobile phase (H_2O/CH_3CN) containing 0.2% of formic acid. Mass spectrometric detection was performed in full-scan mode from *m/z* 50 to 2500, scan time 0.1 s in positive ion mode, ESI spray voltage 4500 V, nitrogen gas 35 psi, drying gas flow rate 11.5 mL min^{-1}, fragmentor voltage 30 V. Almost all the synthesized compounds were analyzed employing method A, compounds analyzed with method B are specified. High-resolution MS (HRMS) ESI analyses were performed on a LTQ Orbitrap XL (Thermo Scientific) mass spectrometer. Melting point (mp) measurements were performed on a Bibby Stuart Scientific SMP3 apparatus. Flash chromatography purifications were carried out using VWR silica gel (40–63 μm particle size). Thin-layer chromatography was performed on Merck 60 F254 plates.

4.1.2. General procedure for the synthesis of 3-hydroxy-1,2-dioxanes 3

The appropriate alkene **2** (8.5 mmol) was added at room temperature to a mixture of the desired β-keto ester **1** (2 equiv.), $Mn(OAc)_3 \cdot 2(H_2O)$ (5 mol%), and $Mn(OAc)_2 \cdot 4(H_2O)$ (5 mol%) in acetic acid (2 mL/mmol). The resulting homogeneous solution was stirred at room temperature for 4 h under oxygen at atmospheric pressure (O_2 filled balloon) and the conversion was monitored by TLC. The reaction mixture was neutralized with NaOH (6 M aqueous solution, 50 mL) and then made slightly basic by adding saturated $NaHCO_3$ solution. The aqueous phase was extracted with EtOAc (3 × 25 mL), the combined organic phases were dried (Na_2SO_4) and the solvent evaporated to dryness under reduced pressure. 3-Hydroxy-1,2-dioxanes **3** were purified by flash chromatography on silica gel or by recrystallization.

*4.1.2.1. Methyl 6,6-dibutyl-3-hydroxy-3-methyl-1,2-dioxane-4-carboxylate (**3a**).* Mobile phase for the chromatographic purification: cyclohexane/ethyl acetate = 9/1 to 7/3.70% yield. ^{1}H NMR (400 MHz, $CDCl_3$) δ 3.74 (s, 3H), 2.92 (dd, J = 13.1, 5.0 Hz, 1H), 2.09 (dd, J = 14.0, 13.1 Hz, 1H), 1.91–1.79 (m, 1H), 1.75 (dd, J = 14.0, 5.0 Hz, 1H), 1.62–1.13 (m, 11H), 1.49 (s, 3H), 0.96–0.87 (m, 6H). ^{13}C NMR (100 MHz, $CDCl_3$) δ 172.1, 97.8, 81.2, 52.0, 44.5, 36.0, 30.8, 30.4, 25.3, 24.7, 24.2, 23.0, 23.0, 13.9, 13.8. HPLC (method B)-LRMS (ESI) *m/z* 271.2 $[M - H_2O + H]^+$, 306.2 $[M + H_2O]^+$, 372.2 $[M + K]^+$, 599.2 $[2M + Na]^+$, R_t = 9.5 min. HRMS (ESI) *m/z* $[M - H_2O + H]^+$ calcd for $C_{15}H_{27}O_4$: 271.1904, found: 271.1890.

4.1.2.2. Methyl 3-hydroxy-3-methyl-6,6-diphenyl-1,2-dioxane-4-carboxylate (3e). The crude mixture was dissolved in the minimum amount of CH_2Cl_2/MeOH mixture and the pure product was crystallized by adding cold cyclohexane. 78% yield. Mp = 168–170 °C. ^{1}H NMR (400 MHz, $CDCl_3$) δ 7.54 (d, J = 8.0 Hz, 1H), 7.40 (t, J = 8.0 Hz, 1H), 7.34–7.21 (m, 8H), 3.75 (s, 3H), 2.93–2.81 (m, 3H), 1.41 (s, 3H). ^{13}C NMR (100 MHz, $CDCl_3$) δ 171.9, 143.1, 140.7, 128.5, 128.4, 128.0, 127.4, 126.7, 125.7, 98.5, 85.2, 52.2, 45.4, 31.8, 24.5. HPLC-LRMS (ESI) *m/z* 311.0 $[M - H_2O + H]^+$, 346.0 $[M + H_2O]^+$, 679.0 $[2M + Na]^+$, R_t = 10.3 min. HRMS (ESI) *m/z* $[M + H_2O]^+$, calcd for $C_{19}H_{22}O_6$: 346.1416, found: 346.1424.

4.1.3. General procedure for the synthesis of 3-methoxy-1,2-dioxanes 4

(1*S*)-(+)-Camphorsulfonic acid (15 mol%) was added at room temperature to a solution of the desired 3-hydroxy-1,2-dioxane **3** (5.72 mmol) in anhydrous methanol (2 mL/mmol). The mixture was stirred at 65 °C for 24 h. The conversion was monitored by TLC. Then, the solvent was removed under reduced pressure and DCM (15 mL) was added. The organic phase was washed at 0 °C with $NaHCO_3$ (saturated aqueous solution, 15 mL), dried (Na_2SO_4) and evaporated to dryness. 3-Methoxy-1,2-dioxanes **4** were isolated after flash chromatography on silica gel.

The assayed product **4a** (*cis* and *trans* isomers) was synthesized following a previously reported procedure [19a] and the spectroscopic data and physical properties of the obtained products were identical to the previously reported ones.

4.1.3.1. Methyl 3-methoxy-3-methyl-6,6-diphenyl-1,2-dioxane-4-carboxylate (4e). Mobile phase for the chromatographic purification: cyclohexane/ethyl acetate = 9/1.47% yield. ^{1}H NMR (400 MHz, $CDCl_3$) δ 7.54 (d, J = 8.0 Hz, 2H), 7.40 (t, J = 8.0 Hz, 2H), 7.34–7.19 (m, 6H), 3.72 (s, 3H), 3.45 (s, 3H), 3.04–2.97 (m, 1H), 2.78–2.70 (m, 2H), 1.36 (s, 3H). ^{13}C NMR (100 MHz, $CDCl_3$) δ 171.1, 143.5, 141.0, 128.4, 128.2, 128.0, 127.3, 127.0, 126.3, 101.2, 85.4, 52.0, 49.2, 46.2, 31.2, 19.4. HPLC-LRMS (ESI) *m/z* 311.0 $[M\text{-}OMe]^+$, 365.0 $[M + Na]^+$, 685.6 $[2M + H]^+$, R_t = 11.2 min. HRMS (ESI) *m/z* $[M + Na]^+$, calcd for $C_{20}H_{22}NaO_5$: 365.1359, found: 365.1368.

4.1.4. General procedure for the synthesis of 4-hydroxymethyl-1,2-dioxanes 5

$LiAlH_4$ (1 equiv) was added at 0 °C to a solution of 3-methoxy-

1,2-dioxane **4** (2.46 mmol) in anhydrous THF (12.5 mL). The mixture was stirred at 0 °C for 1 h (conversion monitored by TLC). The reaction was quenched at 0 °C with $NaHCO_3$ (saturated aqueous solution, 15 mL), the THF was dried under reduced pressure and the mixture was extracted with EtOAc (3 × 15 mL). The organic phases were collected, dried (Na_2SO_4) and evaporated to dryness. 4-Hydroxymethyl-1,2-dioxanes **5** were isolated after flash chromatography on silica gel. The chromatographic purification allowed to separate *cis* and *trans* isomers of the products **5**.

4.1.4.1. (6,6-Dibutyl-3-methoxy-3-methyl-1,2-dioxan-4-yl)methanol (5a). Mobile phase for the chromatographic purification: cyclohexane/diethyl ether = 1/1.96% yield.

Cis-**5a**: ^{1}H NMR (400 MHz, $CDCl_3$) δ 3.89 (dd, *J* = 11.5, 3.1 Hz, 1H), 3.53 (dd, *J* = 11.6, 3.7 Hz, 1H), 3.34 (s, 3H), 2.05 (t, *J* = 12.0 Hz, 1H), 1.97–1.86 (m, 2H), 1.55–1.16 (m, 12H), 1.35 (s, 3H), 0.94–0.88 (m, 6H). ^{13}C NMR (100 MHz, $CDCl_3$) δ 103.2, 81.8, 62.9, 48.5, 39.8, 36.3, 31.4, 29.8, 25.4, 24.8, 23.2, 23.2, 18.8, 14.0, 13.9. HPLC (method B)-LRMS (ESI) *m/z* 243.0 $[M\text{-}OMe]^+$, 257.2 $[M - H_2O + H]^+$, 297.2 $[M + Na]^+$, 313.0 $[M + K]^+$, 571.0 $[2M + Na]^+$, R_t = 9.1 min. HRMS (ESI) *m/z* $[M + Na]^+$, calcd for $C_{15}H_{30}NaO_4$: 297.2036, found: 297.2048.

Trans-**5a**: ^{1}H NMR (400 MHz, $CDCl_3$) δ 3.64 (dd, *J* = 10.6, 8.8 Hz, 1H), 3.54 (dd, *J* = 10.7, 5.9 Hz, 1H), 3.37 (s, 3H), 2.33–2.17 (m, 1H), 1.76–1.64 (m, 1H), 1.64 (dd, *J* = 13.3, 3.5 Hz, 1H), 1.28 (s, 3H), 1.57–1.10 (m, 12H), 0.91 (t, *J* = 7.2 Hz, 3H), 0.90 (t, *J* = 7.2 Hz, 3H). ^{13}C NMR (100 MHz, $CDCl_3$) δ 106.8, 84.2, 62.7, 49.1, 41.6, 36.6, 32.7, 32.6, 25.5, 25.4, 23.2, 23.1, 14.1, 13.9, 13.9. HPLC (method B)-LRMS (ESI) *m/z* 257.2 $[M - H_2O + H]^+$, 297.2 $[M + Na]^+$, 313.2 $[M + K]^+$, 571.2 $[2M + Na]^+$, R_t = 8.5 min. HRMS (ESI) *m/z* $[M + Na]^+$, calcd for $C_{15}H_{30}NaO_4$: 297.2036, found: 297.2056.

4.1.4.2. (3-Methoxy-3-methyl-6,6-diphenyl-1,2-dioxan-4-yl)methanol (5e). Mobile phase for the chromatographic purification: cyclohexane/EtOAc = 8/2.88% yield.

Cis-**5e**: ^{1}H NMR (400 MHz, $CDCl_3$) δ 7.54 (d, *J* = 7.2 Hz, 2H), 7.37 (d, *J* = 7.2 Hz, 2H), 7.29–7.16 (m, 6H), 3.87 (dd, *J* = 3.6, 11.6 Hz, 1H), 3.61 (dd, *J* = 4.0, 11.6 Hz, 1H), 3.45 (s, 3H), 2.81 (dd, *J* = 13.2, 14.0 Hz, 1H), 2.52 (dd, *J* = 4.0, 14.0 Hz, 1H), 1.85 (dq, *J* = 3.6, 12.8 Hz, 1H), 1.23 (s, 3H). ^{13}C NMR (100 MHz, $CDCl_3$) δ 144.2, 141.8, 128.3, 128.2, 127.8, 127.1, 127.0, 126.1, 103.8, 86.1, 62.9, 48.9, 41.0, 31.4, 18.7. HPLC-LRMS (ESI) *m/z* 297.0 $[M - H_2O + H]^+$, 337.0 $[M + Na]^+$, 353.0 $[M + K]^+$, R_t = 6.6 min. HRMS (ESI) *m/z* $[M + Na]^+$, calcd for $C_{19}H_{22}NaO_4$: 337.1410, found: 337.1402.

4.1.5. General procedure for the synthesis of intermediate 4-carbaldehyde-1,2-dioxanes 6

Alcohol **5** (0.3 mmol) was dissolved in anhydrous CH_2Cl_2 (2.5 mL/mmol) and Dess–Martin periodinane (1.05 equiv.) was added at 0 °C. The solution was stirred at room temperature for 1 h (conversion monitored by TLC). The solvent was removed under reduced pressure and the crude was directly purified by flash chromatography on silica gel (mobile phase: cyclohexane/EtOAc = 9/1). The intermediate aldehyde **6** was immediately used in the subsequent step. For further details on this transformation, see Supporting Information.

4.1.6. General procedure for the synthesis of 4-aminopropyl derivatives 8f-l (reductive amination)

Aldehyde **6** (0.2 mmol) was dissolved in anhydrous MeOH (2 mL) and the desired amine **7** (1 equiv.) was added. The reaction was stirred at room temperature overnight. The solution was then cooled to 0 °C and $NaBH_4$ (1.5 equiv.) was added. The reaction mixture was further stirred at room temperature for 1.5 h and quenched with H_2O (5 mL). The organic solvent was removed under reduced pressure and the aqueous phase was extracted with AcOEt (3 × 5 mL). The combined organic phases were dried over Na_2SO_4 and evaporated under reduced pressure. The desired 4-aminopropyl derivatives **8f-l** were obtained pure after purification by flash-chromatography on silica gel. For details on the synthesis of amines **7**, see Supporting Information.

The assayed products **8a-e** were synthesized following a previously reported procedure [19d] and the spectroscopic data and physical properties of the obtained products were identical to the previously reported ones.

4.1.6.1. N-((6,6-dibutyl-3-methoxy-3-methyl-1,2-dioxan-4-yl)methyl)-3-(1H-1,2,4-triazol-1-yl)propan-1-amine (8f). Mobile phase for the chromatographic purification: CH_2Cl_2/MeOH = 9/1.^{1}H NMR (400 MHz, $CDCl_3$) δ 8.03 (s, 1H), 7.89 (s, 1H), 4.24 (t, *J* = 6.8 Hz, 2H), 3.24 (s, 3H), 2.68 (dd, *J* = 4.0, 12.0 Hz, 1H), 2.53 (t, *J* = 6.8 Hz, 2H), 2.46 (dd, *J* = 8.0, 11.6 Hz, 1H), 2.00 (quintet, *J* = 6.8 Hz, 2H), 1.95–1.81 (m, 2H), 1.60 (t, *J* = 12.8 Hz, 1H), 1.52–1.35 (m, 3H), 1.35–1.15 (m, 9H), 1.25 (s, 3H), 0.90–0.84 (m, 6H). ^{13}C NMR (100 MHz, $CDCl_3$) δ 151.8, 143.0, 102.1, 81.8, 50.6, 48.5, 47.2, 46.4, 39.2, 36.3, 32.1, 31.4, 29.7, 25.4, 24.8, 23.2, 18.9, 14.0, 13.9. HPLC-LRMS (ESI) *m/z* 383.2 $[M + H]^+$, R_t = 9.6 min. HRMS (ESI) *m/z* $[M + H]^+$, calcd for $C_{20}H_{39}N_4O_3$: 383.3017, found: 383.3025.

*4.1.6.2. 3-(1H-imidazol-1-yl)–N-((3-methoxy-3-methyl-6,6-diphenyl-1,2-dioxan-4-yl)methyl)propan-1-amine (**8g**).* Mobile phase for the chromatographic purification: CH_2Cl_2/MeOH = 9/1.^{1}H NMR (400 MHz, $CDCl_3$) δ 7.57 (d, *J* = 6.8 Hz, 2H), 7.49 (s, 1H), 7.42 (d, *J* = 7.2 Hz, 2H), 7.33–7.20 (m, 6H), 7.07 (s, 1H), 6.93 (s, 1H), 4.06 (t, *J* = 6.8 Hz, 2H), 3.45 (s, 3H), 2.77 (dd, *J* = 4.0, 12.0 Hz, 1H), 2.73 (dd, *J* = 13.6, 4.0 Hz, 1H), 2.64–2.57 (m, 1H), 2.59 (t, *J* = 6.8 Hz, 2H), 2.49 (t, *J* = 12.4 Hz, 1H), 1.95 (quintet, *J* = 6.8 Hz, 2H), 1.90–1.83 (m, 1H), 1.21 (s, 3H). ^{13}C NMR (100 MHz, $CDCl_3$) δ 144.4, 141.8, 137.1, 129.3, 128.2, 128.1, 127.6, 127.0, 126.0, 118.8, 102.8, 86.1, 50.3, 48.8, 46.5, 44.6, 40.4, 33.5, 31.1, 18.6. HPLC-LRMS (ESI) *m/z* 422.2 $[M + H]^+$, 444.2 $[M + Na]^+$, R_t = 6.8 min. HRMS (ESI) *m/z* $[M + H]^+$, calcd for $C_{25}H_{32}N_3O_3$: 422.2438, found: 422.2446.

4.1.6.3. N-((3-butyl-3-methoxy-6,6-diphenyl-1,2-dioxan-4-yl)methyl)-3-(1H-imidazol-1-yl)propan-1-amine (8h). Mobile phase for the chromatographic purification: CH_2Cl_2/MeOH = 9/1.^{1}H NMR (400 MHz, $CDCl_3$) δ 7.54 (d, *J* = 7.3 Hz, 2H), 7.50 (s, 1H), 7.37 (t, *J* = 7.5 Hz, 2H), 7.30–7.20 (m, 6H), 7.05 (s, 1H), 6.92 (s, 1H), 4.05 (t, *J* = 6.8 Hz, 2H), 3.41 (s, 3H), 2.80–2.72 (m, 2H), 2.66–2.51 (m, 3H), 2.12–1.96 (m, 3H), 1.67 (ddd, *J* = 15.6, 10.7, 5.4 Hz, 1H), 1.55 (ddd, *J* = 5.6, 11.2, 16.8 Hz, 1H), 1.15–1.03 (m, 2H), 0.98–0.82 (m, 3H), 0.73 (t, *J* = 7.3 Hz, 3H). ^{13}C NMR (100 MHz, $CDCl_3$) δ 144.1, 141.8, 137.1, 130.0, 129.2, 128.2, 128.1, 127.6, 127.0, 126.9, 126.1, 118.8, 104.1, 86.0, 49.8, 48.3, 46.5, 44.6, 35.5, 33.2, 31.5, 31.1, 25.6, 22.6, 13.6. HPLC-LRMS (ESI) *m/z* 464.2 $[M + H]^+$, R_t = 8.8 min. HRMS (ESI) *m/z* $[M + H]^+$, calcd for $C_{28}H_{38}N_3O_3$: 464.2908, found: 464.2900.

4.1.6.4. N-((6,6-bis(4-fluorophenyl)-3-methoxy-3-methyl-1,2-dioxan-4-yl)methyl)-3-(1H-imidazol-1-yl)propan-1-amine (8i). Mobile phase for the chromatographic purification: CH_2Cl_2/MeOH = 9/1.^{1}H NMR (400 MHz, $CDCl_3$) δ 7.48 (dd, *J* = 8.6, 5.4 Hz, 3H), 7.16 (dd, *J* = 8.8, 5.4 Hz, 2H), 7.08 (t, *J* = 8.7 Hz, 3H), 6.93 (t, *J* = 8.7 Hz, 3H), 4.04 (t, *J* = 6.7 Hz, 2H), 3.40 (s, 3H), 2.75 (dd, *J* = 12.0, 3.9 Hz, 1H), 2.67–2.52 (m, 4H), 2.43 (t, *J* = 13.6 Hz, 1H), 1.95 (quintet, *J* = 6.9 Hz, 2H), 1.79 (ddd, *J* = 16.0, 8.0, 3.9 Hz, 1H), 1.19 (s, 3H). ^{13}C NMR (100 MHz; $CDCl_3$) δ 162.1 (d, *J* = 246.0 Hz), 161.9 (d, *J* = 244.0 Hz), 139.9 (d, *J* = 4.0 Hz), 137.3 (d, *J* = 3.0 Hz), 137.1 (bs), 129.5 (bs), 128.8 (d, *J* = 8.0 Hz), 128.1 (d, *J* = 8.0 Hz), 118.8 (bs), 115.3 (d, *J* = 21.3 Hz), 115.0 (d, *J* = 21.4 Hz), 102.7, 85.4, 50.1, 48.9, 46.5, 40.1, 33.8, 30.6, 29.7, 18.6. HPLC-LRMS (ESI) *m/z* 458.2 $[M + H]^+$,

$R_t = 1.7$ min (broad peak). HRMS (ESI) *m/z* $[M + H]^+$, calcd for $C_{25}H_{30}F_2N_3O_3$: 458.2250, found: 458.2240.

*4.1.6.5. 3-(1H-imidazol-1-yl)–N-(((1R,5S)-6′-methoxy-6,6,6′-trimethylspiro[bicyclo[3.1.1]heptane-2,3′-[1,2]dioxan]-5′-yl)methyl) propan-1-amine (**8j**).* Mobile phase for the chromatographic purification: CH_2Cl_2/MeOH/NH_4OH = 9/1/0.01. By means of the chromatographic purification we were able to separate the 3,4-*cis* products **8j** from the 3,4-*trans* ones **8k**, whereas the mixtures of compounds sharing the same 3,4 relative configuration remained inseparable. The product **8j** was assayed as mixture of 4 diastereoisomers (as shown by OMe signals in the ^{1}H NMR spectrum), characterized by the 3,4-*cis* configuration. However, it was not possible to precisely determine the diastereomeric ratio, because both the ^{1}H NMR and UV/MS-HPLC signals were largely overlying. The identity of the product was confirmed by MS analysis. HPLC-LRMS (ESI) *m/z* 378.2 $[M + H]^+$, 400.2 $[M + Na]^+$, 416.2 $[M + K]^+$, R_t = 5.5–7.0 min. HRMS (ESI) *m/z* $[M + H]^+$, calcd for $C_{21}H_{36}N_3O_3$: 378.2751, found: 378.2762.

*4.1.6.6. 3-(1H-imidazol-1-yl)–N-(((1R,5S)-6′-methoxy-6,6,6′-trimethylspiro[bicyclo[3.1.1]heptane-2,3′-[1,2]dioxan]-5′-yl)methyl) propan-1-amine (**8k**).* Mobile phase for the chromatographic purification: CH_2Cl_2/MeOH/NH_4OH = 9/1/0.01. By means of the chromatographic purification we were able to separate the 3,4-*cis* products **8j** from the 3,4-*trans* ones **8k**, whereas the mixtures of compounds sharing the same 3,4 relative configuration remained inseparable. The product **8k-A** was assayed as mixture of 4 diastereoisomers (as shown by OMe signals in the ^{1}H NMR spectrum), characterized by the 3,4-*trans* configuration. However, it was not possible to precisely determine the diastereomeric ratio, because both the ^{1}H NMR and UV/MS-HPLC signals were largely overlying. The product **8k-B** was assayed as mixture of 3 diastereoisomers (as shown by OMe signals in the ^{1}H NMR spectrum), characterized by the 3,4-*trans* configuration. However, it was not possible to precisely determine the diastereomeric ratio, because both the ^{1}H NMR and UV/MS-HPLC signals were largely overlying. The identity of the product was confirmed by MS analysis. HPLC (method B)-LRMS (ESI) *m/z* 378.2 $[M + H]^+$, 400.2 $[M + Na]^+$, R_t = 1.1 min. HRMS (ESI) *m/z* $[M + H]^+$, calcd for $C_{21}H_{36}N_3O_3$: 378.2751, found: 378.2765.

4.1.6.7. N-((6,6-dibutyl-3-methoxy-3-methyl-1,2-dioxan-4-yl) methyl)-3-(1H-imidazol-1-yl)propan-1-amine (8l). Mobile phase for the chromatographic purification: CH_2Cl_2/MeOH = 9/1.^{1}H NMR (400 MHz, $CDCl_3$) δ 7.54 (s, 1H), 7.06 (s, 1H), 6.94 (s, 1H), 4.07 (t, J = 6.8 Hz, 2H), 3.35 (s, 3H), 2.74 (dd, J = 11.8, 7.2 Hz, 1H), 2.65 (t, J = 6.7 Hz, 2H), 2.47 (dd, J = 11.7, 7.3 Hz, 1H), 2.20–1.9 (m, 3H), 1.75 (dd, J = 13.4, 3.4 Hz, 1H), 1.71–1.63 (m, 1H), 1.54–1.39 (m, 3H), 1.36–1.12 (m, 12H), 0.93–0.87 (m, 6H). ^{13}C NMR (100 MHz, $CDCl_3$) δ 137.2, 129.3, 117.8, 107.0, 84.3, 50.3, 49.2, 46.3, 44.6, 44.6, 39.5, 36.7, 32.7, 31.2, 25.6, 25.4, 23.2, 23.2, 14.3, 14.0, 13.9. HPLC (method B)-LRMS (ESI) *m/z* 350.2 $[M\text{-}OMe]^+$, 382.2 $[M + H]^+$, R_t = 3.5 min. HRMS (ESI) *m/z* $[M + H]^+$, calcd for $C_{21}H_{40}N_3O_3$: 382.3064, found: 382.3053.

4.1.7. General procedure for the synthesis of 4-propargyl ethers 9

Alcohol **5** (0.26 mmol) was dissolved in anhydrous THF (1 mL) and the temperature was decreased to 0 °C. NaH (1.1 equiv.) was added and the mixture was stirred at 0 °C for 1 h. Then, propargyl bromide (1.2 equiv.) was added and the solution was stirred at room temperature overnight (conversion monitored by TLC). The reaction was quenched with NH_4Cl (saturated aqueous solution, 3 mL) and the mixture was extracted with EtOAc (3 × 4 mL). The combined organic phases were dried over Na_2SO_4 and evaporated under reduced pressure. The desired 4-propargyl ethers **9** were obtained pure after purification by flash-chromatography on silica gel (mobile phase: cyclohexane/EtOAc = 9/1 to 7/3). The intermediate ethers **9** were immediately used in the subsequent step. The not converted alcohols **5** were recovered during the chromatographic purification. For further details on this transformation, see Supporting Information.

4.1.8. General procedure for the synthesis of 4-triazolyl ether derivatives 8m-q (click cycloaddition)

Propargyl ether **9** (0.14 mmol) was dissolved in anhydrous CH_2Cl_2 (1 mL). The selected azide **10** (1 equiv.) and $Cu(PPh_3)_3Br$ (10 mol%) were added. The mixture was stirred at room temperature overnight (conversion monitored by TLC). The crude reaction was directly purified by flash-chromatography on silica gel (mobile phase: CH_2Cl_2/MeOH = 9/1) furnishing the pure products **8m-q**. The not converted ether **9** and azide **10** were recovered during the chromatographic purification. For details on the synthesis of azides **10**, see Supporting Information.

*4.1.8.1. 1-(4-(((6,6-dibutyl-3-methoxy-3-methyl-1,2-dioxan-4-yl) methoxy)methyl)-1H-1,2,3-triazol-1-yl)-2-(2,4-difluorophenyl)-3-(1H-1,2,4-triazol-1-yl)propan-2-ol (**8m**).* Mobile phase for the chromatographic purification: CH_2Cl_2/MeOH/NH_4OH = 9/1/0.01.^{1}H NMR (400 MHz, $CDCl_3$) δ 7.98 (s, 1H), 7.84 (s, 1H), 7.62 (s, 1H), 7.43 (ddd, J = 9.8, 8.3, 6.0 Hz, 1H), 6.79 (m, 2H), 5.38 (s, 1H), 4.89 (d, J = 14.2 Hz, 1H), 4.82 (dd, J = 14.1, 1.8 Hz, 1H), 4.70 (dd, J = 14.3, 1.4 Hz, 1H), 4.59 (d, J = 12.0 Hz, 1H), 4.55 (d, J = 16.0 Hz, 1H), 4.27 (d, J = 14.2 Hz, 1H), 3.63 (ddd, J = 9.3, 5.8, 2.3 Hz, 1H), 3.27 (s, 3H), 3.21 (dd, J = 9.3, 7.2 Hz, 1H), 2.19–2.11 (m, 1H), 1.92–1.85 (m, 1H), 1.60–1.16 (m, 15H), 0.94–0.88 (m, 6H). ^{13}C NMR (100 MHz, $CDCl_3$) δ 163.1 (dd, J = 251.6, 12.4 Hz), 158.5 (dd, J = 244.0, 11.7 Hz), 152.1, 145.1, 145.1, 130.1 (dd, J = 9.5, 5.3 Hz), 124.5, 124.5, 112.1 (dd, J = 20.9, 3.1 Hz), 104.3 (t, J = 26.5 Hz), 101.4, 81.5, 75.2 (d, J = 4.9 Hz), 71.8, 64.4, 55.8, 54.6, 48.5, 39.2, 36.3, 31.5, 31.5, 25.4, 24.9, 23.2, 19.3, 14.1, 13.9, 1.0. HPLC (method B)-LRMS (ESI) *m/z* 615.2 $[M + Na]^+$, R_t = 11.6 min. HRMS (ESI) *m/z* $[M + Na]^+$, calcd for $C_{29}H_{42}F_2N_6NaO_5$: 615.3077, found: 615.3088.

*4.1.8.2. (3-(4-(((6,6-dibutyl-3-methoxy-3-methyl-1,2-dioxan-4-yl) methoxy)methyl)-1H-1,2,3-triazol-1-yl)propyl)triphenylphosphonium bromide (**8n**).* Mobile phase for the chromatographic purification: CH_2Cl_2/MeOH = 98/2 and then 95/5.^{1}H NMR (400 MHz, $CDCl_3$) δ 8.27 (bs, 1H), 7.84–7.65 (m, 15H), 4.99 (bs, 2H), 4.56 (bs, 2H), 3.88 (m, 2H), 3.69 (m, 1H), 3.30–3.23 (m, 1H), 3.25 (s, 3H), 2.38 (bs, 2H), 2.16 (m, 1H), 1.92–1.83 (m, 1H), 1.75–1.15 (m, 13H), 1.28 (s, 3H), 0.93–0.85 (m, 6H). ^{13}C NMR (100 MHz, CDCl3) δ 144.5 (bs), 135.2 (d, J = 3.0 Hz), 133.6 (d, J = 10.2 Hz), 130.6 (d, J = 12.6 Hz), 125.5 (bs), 117.7 (d, J = 86.5 Hz), 101.5, 81.6, 72.1, 64.4 (bs), 49.1 (d, J = 19.6 Hz), 48.5, 39.2, 36.3, 31.6, 31.5, 25.4, 24.8, 23.3 (d, J = 2.0 Hz), 23.2, 23.2, 19.8 (d, J = 53.3 Hz), 19.2, 14.1, 13.9. HPLC-LRMS (ESI) *m/z* 658.2 $[M - Br]^+$, R_t = 6.9 min. HRMS (ESI) *m/z* $[M - Br]^+$, calcd for $C_{39}H_{53}N_3O_4P$: 658.3768, found: 658.3780.

*4.1.8.3. (3-(4-(((6,6-dibutyl-3-methoxy-3-methyl-1,2-dioxan-4-yl) methoxy)methyl)-1H-1,2,3-triazol-1-yl)propyl)triphenylphosphonium bromide (**8o**).* Mobile phase for the chromatographic purification: CH_2Cl_2/MeOH = 98/2 and then 95/5.^{1}H NMR (400 MHz, $CDCl_3$) δ 8.26 (bs, 1H), 7.85–7.65 (m, 15H), 5.02 (bs, 2H), 4.59 (bs, 2H), 4.00–3.86 (m, 2H), 3.62–3.55 (m, 1H), 3.40–3.34 (m, 1H), 3.29 (s, 3H), 2.44–2.33 (m, 2H), 2.30–2.21 (m, 1H), 1.80 (dd, J = 13.6, 3.5 Hz, 1H), 1.73–1.64 (m, 1H), 1.54–1.09 (m, 12H), 1.25 (s, 3H), 0.92–0.84 (m, 6H). ^{13}C NMR (100 MHz, $CDCl_3$) δ 144.4 (bs), 135.2 (d, J = 3.0 Hz), 133.6 (d, J = 10.0 Hz), 130.6 (d, J = 12.6 Hz), 125.5 (bs), 117.7 (d, J = 86.5 Hz), 106.2, 84.2, 70.3, 64.2, 49.2, 49.0 (d,

$J = 19.6$ Hz), 39.6, 36.7, 33.3, 32.7, 25.5, 25.4, 23.3 (d, $J = 2.0$ Hz), 23.2, 23.2, 19.9 (d, $J = 53.1$ Hz), 14.7, 14.0, 13.9. HPLC-LRMS (ESI) *m/z* 658.2 $[M - Br]^+$, $R_t = 6.5$ min. HRMS (ESI) *m/z* $[M - Br]^+$, calcd for $C_{39}H_{53}N_3O_4P$: 658.3768, found: 658.3777.

*4.1.8.4. (3-(4-(((3-methoxy-3-methyl-6,6-diphenyl-1,2-dioxan-4-yl) methoxy)methyl)-1H-1,2,3-triazol-1-yl)propyl)triphenylphosphonium bromide **(8p)**.* Mobile phase for the chromatographic purification: CH_2Cl_2/MeOH = 9/1.^{1}H NMR (400 MHz, $CDCl_3$) δ 8.30 (bs, 1H), 7.86 (dd, $J = 12.6$, 7.9 Hz, 1H), 7.81–7.72 (m, 9H), 7.71–7.63 (m, 6H), 7.53 (d, $J = 8.0$ Hz, 2H), 7.35 (t, $J = 7.7$ Hz, 2H), 7.26–7.14 (m, 5H), 4.99 (bt, $J = 6.2$ Hz, 2H), 4.58 (d, $J = 12.0$ Hz, 1H), 4.54 (d, $J = 12.0$ Hz, 1H), 3.96–3.86 (m, 2H), 3.69 (dd, $J = 9.36$, 5.40 Hz, 1H), 3.40–3.34 (m, 1H), 3.37 (s, 3H), 2.71 (dd, $J = 13.6$, 3.9 Hz, 1H), 2.39–2.25 (m, 3H), 2.13–2.03 (m, 1H), 1.15 (s, 3H). ^{13}C NMR (100 MHz, $CDCl_3$) δ 144.5, 144.3, 141.8, 135.2 (d, $J = 3.0$ Hz), 133.6 (d, $J = 10.2$ Hz), 130.6 (d, $J = 12.6$ Hz), 128.3, 128.1, 127.5, 127.1, 126.9, 126.0, 125.6, 117.8 (d, $J = 86.5$ Hz), 102.1, 85.7, 71.4, 64.3, 49.0 (d, $J = 19.3$ Hz), 48.7, 40.4, 32.8, 23.4 (d, $J = 3.0$ Hz), 19.7 (d, $J = 53.2$ Hz), 18.9. HPLC-LRMS (ESI) *m/z* 698.2 $[M - Br]^+$, $R_t = 8.5$ min. HRMS (ESI) *m/z* $[M - Br]^+$, calcd for $C_{43}H_{45}N_3O_4P$: 698.3142, found: 698.3161.

*4.1.8.5. (3-(4-(((3-methoxy-3,6,6-trimethyl-1,2-dioxan-4-yl) methoxy)methyl)-1H-1,2,3-triazol-1-yl)propyl)triphenylphosphonium bromide **(8q)**.* Mobile phase for the chromatographic purification: CH_2Cl_2/MeOH = 9/1.^{1}H NMR (400 MHz, $CDCl_3$) δ 8.29 (bs, 1H), 7.84–7.66 (m, 15H), 5.02 (bs, 2H), 4.61–4.53 (m, 2H), 3.99–3.86 (m, 2H), 3.69 (dd, $J = 9.28$, 5.18 Hz, 1H), 3.31–3.24 (m, 1H), 3.25 (s, 3H), 2.44–2.32 (m, 2H), 2.21–2.13 (m, 1H), 1.66–1.55 (m, 2H), 1.35 (s, 3H), 1.29 (s, 3H), 1.15 (s, 3H). ^{13}C NMR (100 MHz, $CDCl_3$) δ 144.5 (bs), 135.2 (d, $J = 3.0$ Hz), 133.6 (d, $J = 10.1$ Hz), 130.6 (d, $J = 12.6$ Hz), 125.5 (bs), 117.7 (d, $J = 86.4$ Hz), 101.3, 77.7, 71.8, 64.3, 49.0 (d, $J = 19.5$ Hz), 48.5, 39.9, 34.5, 27.3, 23.3 (d, $J = 2.4$ Hz), 22.6, 19.8 (d, $J = 53.4$ Hz), 19.1. HPLC-LRMS (ESI) *m/z* 574.2 $[M - Br]^+$, $R_t = 3.8$ min. HRMS (ESI) *m/z* $[M - Br]^+$, calcd for $C_{33}H_{41}N_3O_4P$: 574.2829, found: 574.2820.

4.2. Parasitology

4.2.1. Parasites

Promastigote forms of *L. donovani* reference strain (MHOM/NP/02/BPK282/0cl4), *L. infantum* reference strain (MHOM/TN/80/IPT1), *L. major* reference strain (MHOM/SU/73/5-ASKH) and *L. tropica* reference strain (MHOM/SU/74/K27) were cultured at 26 °C in HOMEM (Gibco Thermo Fisher Scientific Inc., Waltham, USA) with 20% foetal bovine serum (FBS, EuroClone SpA, Milan, Italy) and 1% penicillin-streptomycin (EuroClone SpA).

4.2.2. Cell cultures

Vero cells (kidney of African green monkey epithelial cell line) were cultured at 37 °C in MEM medium with 10% FBS (EuroClone SpA), 1% penicillin-streptomycin (EuroClone SpA), 1% levoglutamine (EuroClone SpA). THP-1 cells (human leukemia monocytic cell line) were cultured at 37 °C in RPMI-1640 (EuroClone SpA) liquid medium supplemented with 10% FBS (EuroClone SpA), 1% levoglutamine (EuroClone SpA), 50 μM Mercaptoethanol (Gibco), 1% penicillin-streptomycin.

4.2.3. Promastigote growth inhibition assay

The late log/stationary phase of promastigotes was diluted in complete HOMEM medium at 10^6 parasites/mL in 96-well plates and the tested compounds were added at a range concentration of 40 μM–1.6 μM. Cells were incubated at 26 °C for 72 h. The anti-leishmanial drug Amphotericin B was employed as standard drug (positive control). Each experiment was carried out in duplicate. To estimate the concentration at which the compounds caused 50% inhibition of growth (IC_{50}), the AlamarBlue assay was employed (Life Technologies, Thermo Fisher Scientific Inc., Waltham, USA). The AlamarBlue assay includes a colorimetric growth indicator based on detection of metabolic activity. Specifically, the system incorporates an oxidation-reduction (REDOX) indicator that fluoresces and changes color in response to chemical reduction of growth medium resulting from cell growth. This method monitors the reducing environment of proliferating cells; the cell permeable resazurin is added (non-fluorescent form, blue color) and, upon entering cells, is reduced to resorufin (fluorescent form, red color) as a result of cellular metabolic activity. Evaluation was performed after adding 20 μL of AlamarBlue to the cell cultures and incubating at 26 °C. The reducing environment was evaluated after 24 h by absorbance measurement at the Multiskan Ascent Plate Reader (Thermo Fisher Scientific Inc.) at 550 nm and 630 nm.

4.2.4. Anti-amastigote assay

Human acute monocytic leukemia cell line (THP1) were infected with *L. donovani* promastigotes for the assessment of the activity of the selected compounds against the amastigote form of *Leishmania* parasite. THP1 cells were put in a 96-well plate (10^5 cells/mL) in complete RPMI-1640 medium and PMA (0.1 μM, Cayman Chemical Company, Ann Arbor, Michigan, USA) was added to obtain cells adherence. Cells were incubated at 37 °C in a 5% CO2 incubator. After 48 h, the medium was replaced with fresh medium containing stationary phase promastigotes that were then phagocytized by THP-1 cells and transformed into amastigotes. After 24 h of incubation, endoperoxides were added, the plates were incubated at 37 °C in a 5% CO2 incubator for 72 h. After incubation, wells were washed, fixed with methanol and stained with Giemsa. Stained cells were visualized by using a Nikon Eclipse E200 light microscope (Nikon, Tokyo, Japan). The infectivity index (% of infected macrophages x average number of amastigotes per macrophage) was defined by counting at least 100 THP1 cells in duplicate cultures.

4.2.5. Cytotoxicity test

Mammalian kidney epithelial cells (Vero cell line) were seeded (10^5/mL) with complete MEM medium in 96-well plates and incubated with endoperoxides. After 72 h of incubation, 20 μL of AlamarBlue reagent was added to each well and further incubated at 37 °C for 24 h. Reduction of resazurin to resorufin was evaluated after 24 h by absorbance measurement at the Multiskan Ascent Plate Reader (Thermo Fisher Scientific Inc.,) at 550 nm and 630 nm. Each experiment was performed in duplicate. The selectivity index (SI) for each compound was determined as the ratio between cytotoxicity (CC_{50}) in Vero cells and activity (IC_{50}) against *Leishmania* promastigotes.

Authors contribution

M. O. performed the anti-promastigote and anti-amastigote assays and the cytotoxicity tests; C. R. synthesized the 1,2-dioxanes; S. V. supervised the bioassays and analyzed the biological results; A. Q., M. L. and C. T. designed the 1,2-dioxanes synthesis and analyzed the synthetic and biological results; A. Q. and M. L. supervised the 1,2-dioxanes synthesis; A. Q. and M.O. prepared the original draft; all authors contributed to writing and reviewing the manuscript; C.T. and S.V. provided financial resources.

Acknowledgments

Acknowledgement for financial support is made to MIUR, Italy

(PRIN 2015 - 20154JRJPP), Fondazione del Monte di Bologna e Ravenna, Italy (Prot. Nr. 349 bis/2016) and University of Bologna, Italy. We thank Mr. G. Sacco and Mrs. L. Speziali for the execution of some synthetic steps.

Appendix A. Supplementary data

Supplementary data to this article can be found online at https://doi.org/10.1016/j.ejmech.2019.02.070.

References

[1] D. Steverding, The history of leishmaniasis, Parasites Vectors 10 (2017) 82. https://doi.org/10.1186/s13071-017-2028-5.

[2] A. Ilari, A. Fiorillo, I. Genovese, G. Colotti, Polyamine-trypanothione pathway: an update, Future Med. Chem. 9 (1) (2017) 61–77. https://doi.org/10.4155/fmc-2016-0180.

[3] J.C. Dujardin, L. Campino, C. Cañavate, J.P. Dedet, L. Gradoni, K. Soteriadou, A. Mazeris, Y. Ozbel, M. Boelaert, Spread of vector-borne diseases and neglect of leishmaniasis, Europe, Emerg. Inf. Disp. 14 (2008) 1013–1018. https://doi.org/10.3201/eid1407.071589.

[4] J. Alvar, I.D. Vélez, C. Bern, M. Herrero, P. Desjeux, J. Cano, J. Jannin, M. den Boer, The WHO Leishmaniasis Control Team, Leishmaniasis worldwide and global estimates of its incidence, PLoS One 7 (2012) e35671. https://doi.org/10.1371/journal.pone.0035671.

[5] L. Gradoni, M. Mokni, MANUAL ON CASE MANAGEMENT AND SURVEILLANCE OF THE LEISHMANIASES IN THE WHO EUROPEAN REGION, 2017.

[6] a) N. Singh, M. Kumar, R.K. Singh, Leishmaniasis: current status of available drugs and new potential drug targets, Asian Pac. J. Trop. Med. 5 (6) (2012) 485–497. https://doi.org/10.1016/S1995-7645(12)60084-4;
b) S.R. Uliana, C.T. Trinconi, A.C. Coelho, Chemotherapy of leishmaniasis: present challenges, Parasitology 145 (4) (2018) 464–480. https://doi.org/10.1017/S0031182016002523;
c) M. Vermeersch, R. Inocêncio da Luz, K. Toté, J.-P. Timmermans, P. Cos, L. Maes, In vitro susceptibilities of *Leishmania donovani* promastigote and amastigote stages to antileishmanial reference drugs: practical relevance of stage-specific differences, Antimicrob. Agents Chemother. 53 (9) (2009) 3855–3859. https://doi.org/10.1128/AAC.00548-09;
d) F. Bruno, G. Castelli, F. Vitale, E. Giacomini, M. Roberti, C. Colomba, A. Cascio, M. Tolomeo, Effects of *trans*-stilbene and terphenyl compounds on different strains of *Leishmania* and on cytokines production from infected macrophages, Exp. Parasitol. 184 (2018) 31–38. https://doi.org/10.1016/j.exppara.2017.11.004.

[7] a) L. Lachaud, N. Bourgeois, M. Plourd, P. Leproho, P. Bastien, M. Ouellette, Parasite susceptibility to amphotericin B in failures of treatment for visceral leishmaniasis in patients coinfected with HIV type 1 and *Leishmania infantum*, Clin. Infect. Dis. 48 (2) (2009) e16–e22. https://doi.org/10.1086/595710;
b) M. Den Boer, R.N. Davidson, Treatment options for visceral leishmaniasis, Exp. Rev. Anti Infect. Ther. 4 (2) (2006) 187–197. https://doi.org/10.1586/14787210.4.2.187;
c) I.A. Rodrigues, A.M. Mazotto, V. Cardoso, R.L. Alves, A.C.F. Amaral, J.R.d.A. Silva, A.S. Pinheiro, A.B. Vermelho, Natural products: insights into leishmaniasis inflammatory response, Mediat. Inflamm. 501 (2015) 835910. https://doi.org/10.1155/2015/835910;
d) S.L. Croft, P. Olliaro, Leishmaniasis chemotherapy–challenges and opportunities, Clin. Microbiol. Infect. 17 (2011) 1478–1483. https://doi.org/10.1111/j.1469-0691.2011.03630.x.

[8] a) A. Ponte-Sucre, F. Gamarro, J.C. Dujardin, M.P. Barrett, R. López-Vélez, R. García-Hernández, A.W. Pountain, R. Mwenechanya, B. Papadopoulou, Drug resistance and treatment failure in leishmaniasis: a 21st century challenge, PLoS Neglected Trop. Dis. 11 (12) (2017) e0006052, https://doi.org/10.1371/journal.pntd.0006052;
b) M. Vanaerschot, S. Huijben, F. Van den Broeck, J.C. Dujardin, Drug resistance in vectorborne parasites: multiple actors and scenarios for an evolutionary arms race, FEMS Microbiol. Rev. 38 (1) (2014) 41–55. https://doi.org/10.1111/1574-6976.12032;
c) S. Hendrickx, G. Boulet, A. Mondelaers, J.C. Dujardin, S. Rijal, L. Lachaud, P. Cos, P. Delputte, L. Maes, Experimental selection of paromomycin and miltefosine resistance in intracellular amastigotes of *Leishmania donovani* and *L. infantum*, Parasitol. Res. 113 (5) (2014) 1875–1881. https://doi.org/10.1007/s00436-014-3835-7;
d) S. Hendrickx, A. Mondelaers, E. Eberhardt, P. Delputte, P. Cos, L. Maes, In vivo selection of paromomycin and miltefosine resistance in *Leishmania donovani* and *L. infantum* in a Syrian hamster model, Antimicrob. Agents Chemother. 59 (2015) 4714–4718. https://doi.org/10.1128/AAC.00707-15.

[9] a) http://www.who.int/leishmaniasis/research/en/ and in particular see: http://www.who.int/leishmaniasis/research/978_92_4_12_949_6_Annex6.pdf?ua=1;
b) K. Seifert, Structures, targets and recent approaches in anti-leishmanial drug discovery and development, Open Med. Chem. J. 5 (2011) 31–39. https://doi.org/10.2174/1874104501105010031;
c) P. Olliaro, S. Darley, R. Laxminarayan, S. Sundar, Cost-effectiveness projections of single and combination therapies for visceral leishmaniasis in Bihar, India, Trop. Med. Int. Health 14 (2009) 918–925. https://doi.org/10.1111/j.1365-3156.2009.02306.x.

[10] WHO, Accelerating Work to Overcome the Global Impact of Neglected Tropical Diseases: a Roadmap for Implementation. WHO/HTM/NTD/2012, World Health Organization, Geneva, Switzerland, 2012. http://www.who.int/neglected_diseases/NTD_RoadMap_2012_Fullversion.pdf.

[11] J.N. Burrows, R.L. Elliott, T. Kaneko, C.E. Mowbrayd, D. Waterson, The role of modern drug discovery in the fight against neglected and tropical diseases, Med. Chem. Commun. 5 (2014) 688–700. https://doi.org/10.1039/C4MD00011K.

[12] C. Shi Ni Loo, N. Siu Kei Lam, D. Yu, X.-z. Su, F. Lu, Artemisinin and its derivatives in treating protozoan infections beyond malaria, Pharmacol. Res. 117 (2017) 192–217. https://doi.org/10.1016/j.phrs.2016.11.012.

[13] a) WHO, reportWorld Malaria Report 2013, ISBN: 9 789241 56469 4. b) WHO, Guidelines for the Treatment of Malaria, second ed., World Health Organization, Geneva, Switzerland, 2010. http://whqlibdoc.who.int/publications/2010/9789241547925_eng.pdf.

[14] S. Appalasamy, K.Y. Lo, S.J. Ch'ng, K. Nornadia, A.S. Othman, L.-K. Chan, Antimicrobial activity of artemisinin and precursor derived from in vitro plantlets of *Artemisia annua* L, BioMed Res. Int. 2014 (2014) 215872. https://doi.org/10.1155/2014/215872.

[15] S. Roy, R. He, A. Kapoor, M. Forman, J.R. Mazzone, G.H. Posner, R. Arav-Boger, Inhibition of human cytomegalovirus replication by artemisinins: effects mediated through cell cycle modulation, Antimicrob. Agents Chemother. 59 (7) (2015) 3870–3879. https://doi.org/10.1128/AAC.00262-15.

[16] a) R. Sen, S. Bandyopadhyay, A. Dutta, G. Mandal, S. Ganguly, P. Saha, M. Chatterjee, Artemisinin triggers induction of cell-cycle arrest and apoptosis in *Leishmania donovani* promastigotes, J. Med. Microbiol. 56 (9) (2007) 1213–1218. https://doi.org/10.1099/jmm.0.47364-0;
b) M.Y. Want, M. Islamuddin, G. Chouhan, H.A. Ozbak, H.A. Hemeg, A.K. Dasgupta, A.P. Chattopadhyay, F. Afrin, Therapeutic efficacy of artemisinin-loaded nanoparticles in experimental visceral leishmaniasis, Colloids Surfaces B Biointerfaces 130 (2015) 215–221. https://doi.org/10.1016/j.colsurfb.2015.04.013;
c) F. Ghaffarifar, F.E. Heydari, A. Dalimi, Z.M. Hassan, M. Delavari, H. Mikaeiloo, Evaluation of apoptotic and antileishmanial activities of artemisinin on promastigotes and BALB/C mice infected with *leishmania major*, Iran, J. Parasitol. 10 (2) (2015) 258–267.

[17] a) J.M. Mutiso, J.C. Macharia, M. Barasa, E. Taracha, A.J. Bourdichon, M.M. Gicheru, In vitro and in vivo antileishmanial efficacy of a combination therapy of diminazene and artesunate against *Leishmania donovani* in BALB/c mice, Rev. do Inst. Med. Trop. São Paulo 53 (3) (2011) 129–132. https://doi.org/10.1590/S0036-46652011000300003;
b) Y.V. Mishina, S. Krishna, R.K. Haynes, J.C. Meade, Artemisinins inhibit *Trypanosoma cruzi* and *Trypanosoma brucei* rhodesiense in vitro growth, Antimicrob. Agents Chemother. 51 (5) (2007) 1852–1854. https://doi.org/10.1128/AAC.01544-06;
c) C. Chollet, B. Crousse, C. Bories, D. Bonnet-Delpon, P.M. Loiseau, In vitro antileishmanial activity of fluoro-artemisinin derivatives against *Leishmania donovani*, Biomedi, Pharma 62 (7) (2008) 462–465. https://doi.org/10.1016/j.biopha.2008.04.003.

[18] S. Cortes, A. Albuquerque, L.I. Cabral, L. Lopes, L. Campino, M.L. Cristiano, In vitro susceptibility of *Leishmania infantum* to Artemisinin derivatives and selected trioxolanes, Antimicrob, Agents Chemother 59 (8) (2015) 5032–5035. https://doi.org/10.1128/AAC.00298-15.

[19] a) M. Persico, A. Quintavalla, F. Rondinelli, C. Trombini, M. Lombardo, C. Fattorusso, V. Azzarito, D. Taramelli, S. Parapini, Y. Corbett, G. Chianese, E. Fattorusso, O. Taglialatela-Scafati, A new class of antimalarial dioxanes obtained through a simple two-step synthetic approach: rational design and Structure–Activity relationship studies, J. Med. Chem. 54 (2011) 8526–8540. https://doi.org/10.1021/jm201056j;
b) M. Persico, S. Parapini, G. Chianese, C. Fattorusso, M. Lombardo, L. Petrizza, A. Quintavalla, F. Rondinelli, N. Basilico, D. Taramelli, C. Trombini, E. Fattorusso, O. Taglialatela-Scafati, Further optimization of plakortin pharmacophore: structurally simple 4-oxymethyl-1,2-dioxanes with promising antimalarial activity, Eur. J. Med. Chem. 70 (2013) 875–886. https://doi.org/10.1016/j.ejmech.2013.10.050;
c) M. Lombardo, D.P. Sonawane, A. Quintavalla, C. Trombini, D.D. Dhavale, D. Taramelli, Y. Corbett, F. Rondinelli, C. Fattorusso, M. Persico, O. Taglialatela-Scafati, Optimized synthesis and antimalarial activity of 1,2-Dioxane-4-carboxamides, Eur. J. Org. Chem. (2014) 1607–1614. https://doi.org/10.1002/ejoc.201301394;
d) D.P. Sonawane, M. Persico, Y. Corbett, G. Chianese, A. Di Dato, C. Fattorusso, O. Taglialatela-Scafati, D. Taramelli, C. Trombini, D.D. Dhavale, A. Quintavalla, M. Lombardo, New antimalarial 3-methoxy-1,2-dioxanes: optimization of cellular pharmacokinetics and pharmacodynamics properties by incorporation of amino and N-heterocyclic moieties at C4, RSC Adv. 5 (2015) 72995–73010. https://doi.org/10.1039/c5ra10785g;
e) D.P. Sonawane, Y. Corbett, D.D. Dhavale, D. Taramelli, C. Trombini, A. Quintavalla, M. Lombardo, D-Glucose-Derived 1,2,4-trioxepanes: synthesis, conformational study, and antimalarial activity, Org. Lett. 17 (2015) 4074–4077. https://doi.org/10.1021/acs.orglett.5b01996;
f) M. Persico, R. Fattorusso, O. Taglialatela-Scafati, G. Chianese, I. de Paola,

L. Zaccaro, F. Rondinelli, M. Lombardo, A. Quintavalla, C. Trombini, E. Fattorusso, C. Fattorusso, B. Farina, The interaction of heme with plakortin and a synthetic endoperoxide analogue: new insights into the heme-activated antimalarial mechanism, Sci. Rep. 7 (2017) 45485. https://doi.org/10.1038/srep45485.

[20] R. Sen, S. Ganguly, P. Saha, M. Chatterjee, Efficacy of artemisinin in experimental visceral leishmaniasis, Int. J. Antimicrob. Agents 36 (2010) 43–49. https://doi.org/10.1016/j.ijantimicag.2010.03.008.

[21] M. Islamuddin, A. Farooque, B.S. Dwarakanath, D. Sahal, F. Afrin, Extracts of *Artemisia annua* leaves and seeds mediate programmed cell death in *Leishmania donovani*, J. Med. Microbiol. 61 (2012) 1709–1718. https://doi.org/10.1099/jmm.0.049387-0.

[22] a) A.Q. Sousa, M.S. Frutuoso, E.A. Moraes, R.D. Pearson, M.M. Pompeu, High-dose oral fluconazole therapy effective for cutaneous leishmaniasis due to *Leishmania* (Vianna) *braziliensis*, Clin. Infect. Dis. 53 (2011) 693–695. https://doi.org/10.1093/cid/cir496;
b) F. V. de O. Prates, M.E.F. Dourado, S.C. Silva, A. Schriefer, L.H. Guimarães, M. das, G.O. Brito, J. Almeida, E.M. Carvalho, P.R.L. Machado, Fluconazole in the treatment of cutaneous leishmaniasis caused by *Leishmania braziliensis*: a randomized controlled trial, Clin. Infect. Dis. 64 (2017) 67–71. https://doi.org/10.1093/cid/ciw662;
c) A.A. Alrajhi, E.A. Ibrahim, E.B. De Vol, M. Khairat, R.M. Faris, J.H. Maguire, Fluconazole for the treatment of cutaneous leishmaniasis caused by *Leishmania major*, N. Engl. J. Med. 346 (2002) 891–895. https://doi.org/10.1056/NEJMoa011882.

[23] a) M.P. Murphy, Targeting lipophilic cations to mitochondria, Biochim. Biophys. Acta 1777 (2008) 1028–1031. https://doi.org/10.1016/j.bbabio.2008.03.029;
b) J.R. Luque-Ortega, P. Reuther, L. Rivas, C. Dardonville, New benzophenone-derived bisphosphonium salts as leishmanicidal leads targeting mitochondria through inhibition of respiratory complex II, J. Med. Chem. 53 (2010) 1788–1798. https://doi.org/10.1021/jm901677h;
c) A. Chakraborty, N.R. Jana, Design and synthesis of triphenylphosphonium functionalized nanoparticle probe for mitochondria targeting and imaging, J. Phys. Chem. C 119 (2015) 2888–2895. https://doi.org/10.1021/jp511870e;
d) J. Zielonka, J. Joseph, A. Sikora, M. Hardy, O. Ouari, J. Vasquez-Vivar, G. Cheng, M. Lopez, B. Kalyanaraman, Mitochondria-targeted triphenylphosphonium-based compounds: syntheses, mechanisms of action, and therapeutic and diagnostic applications, Chem. Rev. 117 (2017) 10043–10120. https://doi.org/10.1021/acs.chemrev.7b00042.

[24] As carried out for C6-butyl endoperoxides (Table 1), the phenyl-substituted synthetic intermediates **3e**, 3,4-*cis* **4e**, and 3,4-*cis* **5e** were tested on promastigotes of *L. donovani* and resulted inactive at 40 μM (see Supporting Information).

[25] a) P.M. O'Neill, V.E. Barton, S.A. Ward, The molecular mechanism of action of artemisinin - the debate continues, Molecules 15 (2010) 1705–1721. https://doi.org/10.3390/molecules15031705;
b) L. Tilley, J. Straimer, N.F. Gnädig, S.A. Ralph, D.A. Fidock, Artemisinin action and resistance in Plasmodium falciparum, Trends Parasitol. 32 (2016) 682–696. https://doi.org/10.1016/j.pt.2016.05.010.

[26] M. Chatterjee, S. De Sarkar, G. Geroldinger, M. Tonner, K. Staniek, L. Gille, Oxidative stress mediated anti-leishmanial activity of endoperoxides represent a new therapeutic strategy in Leishmaniasis, Free Radic. Biol. Med. 120 (2018) S163. https://doi.org/10.1016/j.freeradbiomed.2018.04.537.

[27] a) G. Geroldinger, M. Tonner, W. Fudickar, S. De Sarkar, A. Dighal, L. Monzote, K. Staniek, T. Linker, M. Chatterjee, L. Gille, Activation of anthracene endoperoxides in *leishmania* and impairment of mitochondrial functions, Molecules 23 (2018) 1680. https://doi.org/10.3390/molecules23071680;
b) G. Geroldinger, M. Tonner, H. Hettegger, M. Bacher, L. Monzote, M. Walter, K. Staniek, T. Rosenau, L. Gille, Mechanism of ascaridole activation in *Leishmania*, Biochem. Pharmacol. 132 (2017) 48–62. https://doi.org/10.1016/j.bcp.2017.02.023.